NACA RM E56F11

RESEARCH MEMORANDUM

SURGE-INCEPTION STUDY IN A TWO-SPOOL TURBOJET ENGINE

By Lewis E. Wallner, Robert J. Lubick, and Martin J. Saari

Lewis Flight Propulsion Laboratory
Cleveland, Ohio

NATIONAL ADVISORY COMMITTEE
FOR AERONAUTICS
WASHINGTON

NACA RM E56F11

SURGE-INCEPTION STUDY IN A TWO-SPOOL TURBOJET ENGINE

By Lewis E. Wallner, Robert J. Lubick, and Martin J. Saari

ABSTRACT

Extensive steady-state and transient instrumentation was employed to study compressor behavior leading to surge. Compressor surge in the midspeed region and rotating stall in the low-speed region for the outer spool were avoided by the use of compressor air bleed. For acceleration to the compressor stall limit, it was found that rotating stall was not a necessary condition for compressor surge. For these accelerations, the exit-stage group was first to stall, followed by the stalling of the upstream stages in succession. Individual stage-group stall lines were constructed, and a comparison made with a stall line computed from a steady-state loading curve for one stage group.

INDEX HEADINGS

Engines, Turbojet	3.1.3
Engines, Control - Turbojet	3.2.2
Compressors - Axial Flow	3.6.1.1

NACA RM E56F11

NATIONAL ADVISORY COMMITTEE FOR AERONAUTICS

RESEARCH MEMORANDUM

SURGE-INCEPTION STUDY IN A TWO-SPOOL TURBOJET ENGINE

By Lewis E. Wallner, Robert J. Lubick, and Martin J. Saari

SUMMARY

A two-spool turbojet engine was operated in the Lewis altitude wind tunnel to study the inception of compressor surge. In addition to the usual steady-state pressure and temperature measurements, the compressors were extensively instrumented with fast-response interstage pressure transducers. Thus it was possible to obtain maps for both compressors, pressure oscillations during rotating stall, effects of stall on efficiency, and stage-loading curves. In addition, with the transient measurements, it was possible to record interstage pressures and then compute stage performance during accelerations to the stall limit.

Rotating stall was found to exist at low speeds in the outer spool. Although the stall arose from poor flow conditions at the inlet-stage blade tips, the low-energy air moved through the machine from the tip at the inlet to the outer spool to the hub at the inlet to the inner spool. This tip stall ultimately resulted in compressor surge in the midspeed region, and necessitated intercompressor air bleed.

Interstage pressure measurements during acceleration to the compressor stall limit indicated that rotating stall was not a necessary condition for compressor surge and that, at the critical stall point, the circumferential interstage pressure distribution was uniform. The exit-stage group of the inner spool was first to stall; then, the stages upstream stalled in succession until the inlet stage of the outer spool was stalled. With a sufficiently high fuel rate, the process repeated with a cycle time of about 0.1 second. It was possible to construct reproducible stage stall lines as a function of compressor speed from the stage stall points of several such compressor surges. This transient stall line was checked by computing the stall line from a steady-state stage-loading curve. Good agreement between the stage stall lines was obtained by these two methods.

INTRODUCTION

As the loading of a compressor is increased at a given speed, a point is reached where the flow through the machine is no longer stable. This flow instability, which is generally referred to as surge, is

defined by Stodola (ref. 1), as "a periodic sudden sending back of the compressed fluid through the compressor and into the atmosphere." This loading limit has perplexed designers of both axial- and centrifugal-flow machinery for some time. Throughout the entire period of compressor development, ingenious devices have been suggested to alleviate or circumvent compressor surge. German patents were issued as early as 1915 on methods of reducing the violence of surge by adjusting the discharge volume of a compressor. Other schemes include blade design changes, variable-position stators, air bleed, recirculation, and air-passage modifications (refs. 2 to 7). An efficient compressor can be designed to operate without encountering surge if weight and loading change are unimportant. However, for aircraft applications where efficiency, weight, and acceleration margin are prime considerations, a satisfactory solution to the problem has not been found. The reasons for this are at least twofold: Regardless of the weight or efficiency of an engine, attempts are always being made to improve engine performance in order to improve airplane performance, which generally results in forcing the operating pressures as close to the surge limit as possible. For lack of an adequate signal to warn of the approach of surge, a control that can avoid the dangerous flow instability has not been designed. The problem is complicated by many additional factors such as nonreproducibility of surge data (ref. 8), Reynolds number effects (ref. 9), and inlet distortion effects (ref. 10).

In addition to the classical type of surge defined by Stodola, other flow instabilities can be encountered in compressors (ref. 11). The most widely known of these is the rotating-stall phenomenon, which has been defined as blade flow instability characterized by propagating cells of stalled flow. References 12 to 14 describe these rotating stalls and the conditions at which they are likely to be encountered, how to recognize them, and particularly how to count them. The frequency can be important because of the possibility of excitation of serious blade-vibration stresses (ref. 15).

The advent of high-response instrumentation and high-speed recording techniques provided the means for a closer examination of the surge problem. In an effort to understand the nature of this flow instability, the following are some factors that should be explored: flow conditions existing during surge of the compressor as a unit; the relation between surge and rotating stall; whether surge is simply a magnification of rotating stall; the possibility of the most heavily loaded stage in a compressor causing surge; and prediction of the loading limit of a compressor. In the investigation reported herein these factors are examined by a detailed study of flow conditions within a compressor as surge is approached.

The experimental data presented herein were obtained with a two-spool turbojet engine that had been installed in the Lewis altitude wind tunnel for other research purposes. These data were taken at engine-inlet total pressures corresponding to a flight Mach number of 0.80 at altitudes of

35,000 and 50,000 feet. The compressor units were operated over a range of steady-state pressure ratios well beyond those encountered in normal engine operation by use of air bleed and air injection combined with exhaust-nozzle-area regulation. Interstage measurements were taken to define the steady-state stage performance curves. Fast-response pressure measuring and recording instrumentation provided a method for realizing the following objectives: evaluating stage and over-all compressor performance during transient operation to the stall limit; determining the origin of incipient pressure oscillations within the compressor; tracing the propagation of disturbances through the compressor; constructing stall-limit lines for individual stage groups; and comparing stage stall characteristics determined from transient measurements with a stall line constructed from the steady-state stage-loading curve.

APPARATUS

Engine and Installation

The turbojet engine was mounted on a wing section that spanned the test section of the altitude wind tunnel, as shown in figure 1. Atmospheric air was dried, refrigerated, and throttled to the desired ram pressure ratio before being introduced into the engine through the direct-connected ducting. Automatic, fast-response bleed valves installed in the inlet duct walls were used to keep the ram pressure constant during transient engine operation. (An evaluation of this technique is presented in ref. 16.)

The two-spool engine is in the 10,000-pound-thrust class. The inner-spool unit consists of a seven-stage axial-flow compressor connected to a single-stage turbine. The outer-spool unit consists of a nine-stage axial-flow compressor connected through a concentric shaft to a two-stage turbine. The two units are not coupled mechanically. Two air-bleed ports permit air to be bled from the discharge of the outer spool in order to avoid stall at low engine speeds. In normal engine operation, the bleed valve position is scheduled against corrected outer-spool speed so that the bleed ports are closed at engine speeds above about 90 percent of rated speed. During this investigation, however, the bleed valves were operated manually to facilitate obtaining data over as wide a range of compressor operation as possible.

The normal engine fuel system was replaced by an external system that incorporated a fast-acting fuel throttling valve for making the rapid increases in fuel flow required in the establishment of compressor-surge limits. The valve also provided fuel control during steady-state engine operation.

[redacted]

A clam-shell-type variable-area exhaust nozzle was installed on the engine to provide a method for changing the steady-state operating point of the compressor units and thereby allowed a quasi-steady-state approach to compressor surge.

Instrumentation

Instrumentation used to measure the steady-state compressor performance is indicated in table I. The following parameters were measured on a multiple-channel, direct-inking oscillograph during both steady-state and transient operation: outer- and inner-spool speed, engine fuel flow, inner-spool inlet temperature, and inlet and exit pressures for each compressor. The probes used for these pressures were the visual design used for obtaining steady-state data. As a result, the frequency response of the probe and the complete recording system was flat to only about 10 cycles per second. In order to obtain high-speed records with better frequency-response characteristics, specially designed pressure probes and a different recording method were used. These pressure probes were directly connected to balanced strain-gage transducers, the signal from which was amplified by carrier-type amplifiers. The amplifiers drove galvanometers in a 16-channel photographically recording oscillograph. The frequency response of this measuring system was flat to about 50 cycles per second. Photographic records of the pressure changes could be produced as fast as 48 inches per second. These pressure probes were placed at the exit of compressor stator stages 1, 3, 6, 9, 10, 13, and 16. Although for most of the tests the probes were placed two-thirds the distance from the hub to the tip, the effects of immersion on stall intensity and the effect of circumferential position were investigated.

3941

RESULTS AND DISCUSSION

The purpose of this investigation was to study compressor aerodynamic phenomena over as wide a range of compressor operation as possible. These operating conditions were, in most cases, considerably beyond the constraining limits of normal engine operation with regard to interspool air bleed and exhaust-nozzle variation. Consequently, some of the data bear no relation to the compressor characteristics encountered during normal scheduled engine operation. In order to provide the proper continuity, the steady-state compressor operation, including both over-all and interstage performance, is presented first and is followed by the discussion of compressor operation during fuel flow transients that induce stall or surging conditions.

Steady-State Compressor Performance

Outer spool. - The over-all performance of the outer spool relating pressure ratio, speed, and airflow is shown in figure 2. The effects of

[redacted]

engine exhaust-nozzle-area changes and intercompressor air bleed are illustrated with the stall-limit line (compressor surge). A discussion of the interrelation of these variables in a two-spool turbojet engine is beyond the scope of this paper, but may be found in reference 17. It should be noted that the outer-spool pressure ratio increased with increasing exhaust-nozzle area at a given corrected speed. With the compressor bleeds closed, the steady-state operating line for large nozzle areas can intersect the stall-limit line in the midspeed range. Normally stall-free operation is accomplished by use of interspool air bleed, which lowers the operating pressure ratio below the stall limit. Rotating stall was detected at about 53 percent of outboard-spool rated speed (with bleeds closed), and the rotating stall became progressively more intense as engine speed was increased until, at 67 percent speed, complete stall and surge occurred. It is emphasized that this rotating-stall phenomenon is avoided during scheduled engine operation by using compressor air bleed. The rotating stalls discussed in the following section were purposely induced to study the persistence, propagation, and general behavior characteristics of the rotating-stall phenomena in a full-scale engine.

3941

Interstage pressure oscillations. - Data that indicate the character of the rotating-stall condition (with compressor bleeds closed) in the outer spool are illustrated in figures 2 and 3. Pressure pickups were placed in compressor stages 1, 3, 6, 9, 10, and 13 (at 30-percent immersion) as outlined in the instrumentation discussion. The oscillations in pressure that were obtained through the rotating-stall region are shown in figure 3. Figures 3(a) to (f) correspond to points a to f in figure 2. The pressure traces in figure 3(a) indicate no periodic disturbance and a relatively small amplitude of pressure fluctuation. The amplitude of the pressure oscillations are shown above each pressure trace. As speed is increased to about 57.0 percent (point b, fig. 2) a single rotating stall appears with a pressure amplitude of 5.5 percent in the first compressor stage. This single-zone stall is rotating at about one-half of outer-spool speed (typical for axial-flow compressors) and is rather weak, as evidenced by the short time in stall compared with the unstalled period. Traces from the first stator stage in figure 3(b) indicate a sharp well-defined rotating-stall pattern; however, in the third and sixth stages, the fluctuations have almost disappeared. Farther rearward in the compressor the periodic fluctuations reappear, at the same frequency, although the pattern is less clearly defined. As speed is further increased, a two-zone rotating-stall pattern is formed and the stalled portion of the cycle grows, indicating increased area of the rotating-stall cell. Raising the speed above that for figure 3(e) results in compressor surge; the surge condition persists until the engine is accelerated to about 79.0 percent (point f on fig. 2). Pressure traces at this operating condition (fig. 3(f)) indicate quiescent flow again with relatively small pressure oscillations. For the entire speed range covered, the rotating-stall frequency measured in both compressors was found

to be a function of outer-spool speed, indicating that the stall condition originates in the outer spool.

Compressor efficiency. - Further evidence indicating that the rotating-stall condition originates in the outer spool is provided by the compressor efficiencies presented in figure 4. Outer-spool efficiencies deteriorate rapidly through the rotating-stall speed range, whereas the inner-spool performance remains essentially unaffected. Thus, the periodic stall points b to e (figs. 2 and 3) result from flow conditions in the outer spool. In figure 4 it is evident that some overlap occurs with the bleeds closed at a rotor speed of about 58.0 percent; this stems from a hysteresis effect. The type of compressor operation depends on the direction of speed change; that is, for speed decreased from 67.0 percent, the rotating-stall condition would persist to a speed of perhaps 57.0 percent; however, for speed increased from 50 percent, rotating stall would not be encountered to about 60 percent speed.

The variation of amplitude of pressure oscillations with radial position in rotating stall is shown in figure 5. Pressure oscillations in the rotating-stall speed range were less severe near the hub of the first stator stage. The opposite occurs for the pressure oscillations at the entrance to the inner spool. The hub oscillations are much stronger than those obtained at the tip. Apparently the rotating-stall region originates at the tip of the outer-spool inlet stages, but this low-energy air moves through the compressor into the hub at the inner-spool inlet. This movement of the low-energy air probably explains the weakness of the pressure oscillations in some of the traces in figure 3; that is, the probes, which were in a fixed position at one-third the passage height from the tip, did not detect the strongest stall signals at every stage. However, because the trends in figure 5 are unaffected by speed, the data in figure 3 should be qualitatively representative of speed-change effects in the rotating-stall region.

Inner spool. - The inner-spool map with the air-bleed ports closed is presented in figure 6. Operating lines with two exhaust-nozzle areas and the compressor stall-limit line are shown on the map. Increasing the exhaust-nozzle area lowers the operating line on the inner spool and raises it on the outer spool (see figs. 2 and 6). (See ref. 17 for a discussion of exhaust-nozzle-area effects on a two-spool turbojet engine.) No rotating-stall zones were observed to originate in this compressor during closed-bleed steady-state operation at low engine speeds.

Although the effects of the rotating-stall zones that occurred in the outer spool persisted through the inner spool, no additional rotating-stall zones were found to originate in the inner spool during closed-bleed operation at the low engine speeds. At high rotor speeds, the pressure ratio margin between steady-state and stall operation decreased gradually and thus indicated that, if the rotor-corrected speed were increased sufficiently, a surge condition ultimately would be encountered.

[redacted]

Bleed effect on inner spool. - In the rotor speed range where intercompressor air bleed is effective in relieving outer-spool stall, the effects of this air bleed on the performance of the inner spool are of interest. Intercompressor air bleed reduces the pressure ratio across the outer spool, which in itself would not affect the inner-spool performance. However, air bleed did increase the flow velocity at the tip section of the inner-spool inlet stage by about 10 percent. The radial velocity distortion evidently caused the entire inner-spool map to shift toward lower airflows, as shown in figure 7. Although air bleed normally would not be employed at high rotor speeds, it is of academic interest to note that open-bleed operation at high corrected speeds (about 105 percent) resulted in the formation of an intermittent rotating stall (fig. 7). A high-speed oscillograph trace of the rotating-stall formations is shown in figure 8. At corrected inner-spool speeds as high as 103 percent of rated speed, no rotating-stall patterns are evident (fig. 8(a)); at a corrected speed of 105 percent, an intermittent rotating stall is evident in the thirteenth-stage stator (fig. 8(b)). At a corrected speed of 106.5 percent, the rotating-stall pattern suddenly increases in amplitude, and complete compressor surge occurs (fig. 8(c)). Although this phenomenon has not been generally observed in other compressors at high speeds, it might well be expected; that is, above design speed the excessive pressure ratios in the compressor result in low axial velocities in the rear stages. The low axial velocities in turn mean excessive angle of attack and, hence, rotating-stall formation. Although these stall data are for the compressor bleeds open, at higher altitudes similar stalls were encountered with the bleeds closed. Tests on a three-stage axial-flow compressor, reported in reference 14, also indicate that rotating stalls are formed initially in the outlet stage.

Stage-loading curves. - Stage-loading curves are plotted in figures 9 to 15. In figure 9(a) local pressure coefficients for the tip, mid, and hub stations are shown as functions of average flow coefficient for stage 1 of the outer spool. As is typical for axial-flow compressors, first-stage stall is prevalent at less than design speeds (indicated by the positive slope of the loading curves in the low-speed region). These data indicate that the stall is not localized but rather exists at both the hub and tip stations simultaneously. The rotating stall apparently originated at the tip section, as indicated by the abrupt discontinuity in the characteristic curve of the section. This is further substantiated by the fact that the pressure oscillations shown in figure 5 were most intense at the tip section for the first rotor stage. Therefore the surge condition of the outer spool at rotor speeds between 75 and 84 percent of rated outer-spool speed (fig. 2) is attributable to first-stage tip section characteristic. The pressure coefficient (fig. 9(b)) is plotted as a function of local flow coefficient for stage 1 only, because of insufficient static pressures throughout the compressors to define local flows for all stages. However, at the entrance to the outer spool there was enough instrumentation to compute local flow coefficients at the tip and

[redacted]

hub stations. The local flow data are presented in figure 9(b) as a means of checking the trends indicated by the average flow coefficients in figure 9(a). The curves based on the local flows are similar to the average-flow-coefficient curves except that the flow range at the hub has been broadened considerably and indicates a gentle transition into the stalled region. At the blade tip the entry into stall is more sudden at a corrected speed of about 78 percent (where the bleed-closed operating line intersects the compressor stall line, fig. 2).

An additional picture of the inlet stage performance might be obtained from the first-stage efficiencies, which are shown as a function of rotor speed in figure 9(c). The sharp effect of rotating stall on blade tip efficiency is illustrated by the sudden drop in performance at about 75 percent with the air bleeds closed. Efficiency at the mid and hub stations are not affected strongly by the rotating stall. At the hub the performance deteriorates gradually so that at 50 percent of rated speed the local efficiency is about 40 percent of rated speed efficiency. This is a reflection of the pressure-coefficient data shown in figure 9(b), indicating that the hub is stalled over the greater portion of the speed range.

Loading curves for compressor stages 2 to 3 indicate only small changes for the entire operating range shown (fig. 10). These data are not sufficiently accurate to attach significance to the slope of the mid-span points in figure 10. Compressor stages 4 to 6 (fig. 11) have characteristic shapes of a definite negative slope. This trend becomes more pronounced in the exit group of stages 7 to 9 (fig. 12), where sizeable changes in pressure coefficient occur as flow or engine speed is varied. These loading curves for the outer spool of the engine are typical for a high-pressure-ratio subsonic axial-flow machine (ref. 18).

Pressure-coefficient curves for the inlet stage of the inner spool are presented in figure 13(a). The flow range is small; the outer-spool map (fig. 6) indicates a speed variation of only 28 percent for this compressor. This is contrasted to a speed change of 58 percent for the outer spool (fig. 2). The low level of pressure coefficient indicates light loading of this stage.

The middle group of stages of the inner spool (fig. 14, stages 11 - 13) indicates small changes in flow coefficient (angle of attack), and the relatively high loading is characteristic of this stage group in an axial-flow compressor. The exit-stage-group (fig. 15, stages 14 - 16) loading is characterized by large changes in pressure coefficient for relatively small changes in flow coefficient.

Transient Performance

Comparison of transient and steady-stall limits. - Stall data were obtained on the inner spool by the following techniques:

[redacted]

(1) Slow but steady decreases were made in exhaust-nozzle area until the inner spool was sufficiently loaded to cause surging. For this type of transient data, the direct-inking oscillograph and slow-response pressure probes were used.

(2) Rapid increases were made in engine fuel flow to the surge point. The high-response pressure probes and high-speed recording methods were used to accurately follow pressure changes.

3941

The surge pressure ratios obtained by the two transient-approach techniques were substantiated by obtaining complete over-all and interstage steady-state compressor data at pressure ratios just below the surge point at several engine speeds. This method is commonly used in compressor rig tests where pressure ratio is varied by manipulation of a flow discharge throttle. With an engine, the compressor pressure ratio can be varied similarly by variation of exhaust-nozzle area. The data obtained by these techniques are presented in figure 16, where inner-spool pressure ratio is shown as a function of corrected inner-spool speed. (The inner spool is considered here because this compressor stalled during these transients.) The quasi-static stall points agree favorably (considering the nature of the data) with the fuel-step stall points, which were measured with the fast-response oscillographs. The reliability of both these sets of stall points is attested to by the proximity of the steady-state points obtained under the stall-limit line, which fall reasonably close to the transient data. Rate of approach to the stall-limit line then does not seem to affect the stall pressure ratio.

CA-2

Interstage pressures. - Data for the study of the sequence of events leading to compressor stall during transient operation were obtained from pressure probes at several interstage locations. High-speed oscillograph records of total-pressure variation at the exits of stages 1, 9, and 13 are shown in figure 17. These traces indicate a smooth increase in pressure following the sudden increase in engine fuel flow, with no evidence of rotating-stall formation prior to the peak or stall-inception point. In contrast, the time histories shown in figure 18 illustrate the approach to stall when a rotating stall, with its characteristic pressure oscillations (refs. 12 - 14), existed prior to the step increase in fuel flow. In the case shown, a single-zone stall rotating at about one-half of outer-spool speed existed prior to the beginning of the transient.

It will be recalled that the rotating stall was shown to originate in the outer spool with the air bleeds closed. These pressure traces are from two probes in stator stages 1 and 9 separated circumferentially by about one-third the compressor annulus. It is evident that the rotating-stall patterns are out of phase because of the difference in circumferential position (see arrows F, G, H, L, and K). However, the peak pressures in stage 1 occur at the same time for the two pressures (see point A); also, the minimum pressures (point B) in stage 9 occur at the same time

[redacted]

for the two pressure histories. Between stall point A in stage 1, which is the maximum pressure prior to the collapse, and rotating-stall point H, there is a further deterioration in flow from a single rotating stall to at least a two-zone stall pattern. The significant point demonstrated here is that when the critical stall point (sometimes referred to as stall limit, surge point, full stall, etc.) is reached, the pressure all around the annulus is at its particular maximum.

Adjusting the pressure histories in figure 18(a) for the time difference arising from the rate of travel of the rotating stall and the circumferential location of the probes yields the traces shown in figure 18(b). As would be expected, the rotating-stall patterns are now in phase, but the maximum and minimum points C and D, respectively, are now out of phase. These data would seem to indicate that, for the critical stall point, it is incorrect to adjust the pressure trace for circumferential probe location and that the critical stall pressure is uniform around the annulus even though it was preceded by a rotating-stall condition.

Stage pressures during stall inception. - Typical pressure traces from probes placed in several interstage stations are shown in figure 19. These traces were obtained by step-increasing the fuel flow sufficiently to cause compressor stall with the intercompressor bleeds open (fig. 19 (a)) and closed (fig. 19(b)). The pressure probe in stage 16 indicates the largest increase in pressure prior to the stall. Stall in these figures has been labeled "Region of stall inception" because of the greatly expanded time scale; that is, it would be difficult to select a single point on the time scale as being the compressor stall point. It is interesting to observe the steady and rapid increase in pressure in stage 16 up to a maximum where it "tops-out" (see point A). As this pressure starts to drop, there is a rapid buildup in pressure measured in stator stage 13. A similar action can then be observed in the upstream stages. This action may be explained as follows: At high rotor speeds a sufficiently large fuel input will load the rear stages until one stage stalls. At this instant there is a rapid drop in airflow through the stalled stage and, therefore, the airflow through the remaining stages must decrease to readjust to the new operating condition. As the flow is reduced at essentially constant speed, the angle of attack increases until other stages stall. The time required for a given stage to stall will depend on the flow margin between the operating point and the stall point.

Stage pressure ratios. - From the stage pressure histories obtained during accelerations to compressor stall it is difficult to analyze the significant changes in stage loading. It would be desirable to trace the pressure ratio across the individual stage group during the time the stalling progresses through the machine. Histories of the stage pressure ratios were constructed for all stage groups during the entire acceleration to stall by calibrating the pressure traces and using automatic

computing equipment. In figure 20 are plotted both stage and over-all compressor pressure ratios as functions of time for bleeds open and closed. Prior to the critical stall point A in figure 20, the maximum loading change takes place in exit stages 14 to 16 of the inner spool. It is the outlet stage group (stages 14 to 16) that stalls first, followed in succession by the upstream stages to the inlet of the outer spool. Progression of the stalling process through both compressors requires between 0.02 and 0.03 second. The histories of over-all compressor pressure ratio are similar for both open and closed bleed positions (fig. 20). It is interesting to note that the loading of the outer spool remains essentially unchanged during the entire acceleration, while the inner-spool pressure ratio increases to stall (point G, fig. 20). At this point, the inner spool unloads rapidly, while the outer-spool pressure ratio builds up to the point at which it also stalls (point H, fig. 20). Although stall points A to F in figure 20 occur in an orderly fashion, this sequence need not always be the same. As was discussed in the section "Stage pressures during stall inception," the time required for a given stage to stall will depend on where the stage is operating before the stalling cycle begins. For example, if, when a rear stage stalled (causing a flow readjustment through the machine) stage 9 were operating much closer to its critical flow than stage 13, stage 9 would stall prior to stage 13. Therefore, some stall sequences were observed that were not in the geometric order shown in figure 20.

3941

CA-2 back

Stage stall lines. - Stage stall points or pressure-ratio peaks were obtained for several speeds at 35,000 feet and a flight Mach number of 0.8 from a series of plots such as those in figure 20. These points were then plotted as a function of respective spool speed to form the stage stall lines in figure 21. These stage stall points do not occur simultaneously, but rather in a time sequence as was demonstrated in figure 20. The stall points for a given stage group and compressor-bleed position correlate to a single line in an orderly fashion. The fact that the stage pressure ratio, during an acceleration to the compressor stall limit, rises to a unique value at a given speed and then drops off, confirms that this peak pressure ratio is the stall value for that particular stage group. The locus of these peak pressure ratios obtained during the stall cycle then represents the stall line for that particular stage group.

In addition to the individual stage groups, the stall pressure-ratio points for the inner and outer spool are shown in figure 21. These data also determine well-defined curves. Use of the intercompressor air bleeds has some effect on several of the stall lines. The exact reason for this effect is not known although, as previously noted, air bleed did alter the intercompressor velocity profiles considerably.

The same reduction techniques used to obtain the data in figure 21 were used on stalls run at an altitude of 50,000 feet and a flight Mach number of 0.8. The results obtained at 50,000 feet are similar to those

[redacted]

at the lower altitude. This similarity can be seen by the direct comparison of the stall data for over-all pressure ratio for both compressors shown in figure 22.

Transient and steady-state stall. - From a stage-loading plot of the pressure coefficient against the flow coefficient, it is possible to calculate the stage stall pressure ratio (see appendix). This calculation is feasible because the stage-loading curve is a unique function of pressure and flow coefficients and is unaffected by rotor speed. Therefore, from the peak pressure coefficient on a stage-loading plot the stage stall pressure-ratio curve can be calculated over the desired speed range. A calculated stall line for the outlet-stage group is compared with the transient stall data for this stage group (from fig. 21) in figure 23. This computed steady-state stall line affords an excellent check on the transient stage stall data. This close agreement then leads to the conclusion that transient stage-stall characteristics can be closely predicted from the steady-state pressure coefficient curve, thus affording a method very helpful in predicting how much a compressor can be loaded before the stall-limit pressure ratio is obtained.

Acceleration

Typical accelerations are shown in terms of stage-pressure ratio and corrected speed in figure 24. For the successful throttle bursts (accelerations A and C), the outer spool accelerates in speed along a path very close to its steady-state operating lines. The inner-spool stage groups load in the direction of the respective stage stall line, with the most pronounced loading change in the outlet-stage group. An acceleration to the stall line (acceleration B) produces more far-reaching effects within the compressors. The pressure ratio of the inner-spool outlet group increases to its stall line (reproduced from fig. 21) and then starts to unload. The preceding stages in the inner spool act similarly in sequence. (The point at which the individual stage groups are operating when the last group of the inner spool is at the stall point is marked with a triangular symbol.) The stage stalling then moves into the outer spool and each of these groups load and stall in an orderly sequence through the entire compressor. This action in the outer spool is in sharp contrast to the accelerations that did not encounter stall where the stages hardly deviated from their steady-state operating lines.

CONCLUDING REMARKS

A study was made of the surge inception characteristics of the compressor units of a two-spool turbojet engine. The compressors were representative of current design practices and performed well within the

[redacted]

intended operating regions. Incipient stall and surge conditions were induced by fuel flow and exhaust-nozzle-area variations as well as by off-design operation of compressor bleeds.

Operation at low rotor speeds with compressor bleeds closed resulted in a rotating-stall condition that originated in the blade tip region of the inlet stage of the outer spool. The effect of the rotating stall persisted through both compressors, but the low-energy air in the stall zone propagated from the tip area of the outer-spool inlet stage to the hub area of the inner-spool inlet stage. The tip stall in the outer compressor ultimately degenerated into a complete surge condition in the midspeed region. The flow conditions over the entire blade span were typically off-design for operation with the bleeds closed at low rotor speeds. The stall condition was alleviated by use of intercompressor air bleed. Bleeding of air from between the two compressors upset the velocity distribution into the inner spool, which resulted in a shift of the performance map in the direction of lower airflow. In addition, air bleed gave rise to a rotating-stall condition in the inner spool at high rotor speeds that sometimes resulted in complete surge.

Fast-response instrumentation and high-speed recording techniques were used to show that the rate of approach had no effect on the stall-limit line. Interstage pressure measurements during acceleration to the compressor stall limit indicated that rotating stall was not a necessary condition to compressor surge. At the critical stall point (peak pressure) the circumferential interstage pressure distribution was uniform; if rotating stall existed prior to the start of the acceleration, the pressure around a given stage was varying. However, when the critical stall point was reached, the pressure around the annulus was uniform.

From interstage pressure traces made during surge inception, histories of stage pressure ratios were computed. The outlet group of stages generally was first to stall during an acceleration at high engine speed. With sufficiently rapid pressure traces, it could be seen that following the pressure rise and sharp drop in the rear stage (which signaled stall inception) similar action took place in the upstream stages; that is, in one stage after another there was a sharp increase in pressure and then a sudden collapse. If the excessive fuel rates that caused the acceleration were sufficiently high, the stall would be repeated at a rate of approximately 10 cycles per second (surge). From these stage stall points for a large series of compressor surges, reproducible stage stall lines were constructed as functions of rotor speed.

As a check on the transient stage stall, a stall line was synthesized from a stage-loading curve that was constructed from steady-state data. The transient and steady-state stall lines for the stage group investigated agreed quite closely.

[redacted]

While the results of this investigation add to the clarification of some aspects of the compressor-surge phenomenon, further study is required to provide a concise understanding of the surge inception and propagation process as well as to ascertain the generality of the phenomenon for axial-flow machines. An example of such a problem area would be the definition of the validity of cascade test data in determining multistage compressor stage characteristics, particularly during transient operation.

Lewis Flight Propulsion Laboratory
National Advisory Committee for Aeronautics
Cleveland, Ohio, June 21, 1956

[redacted]

APPENDIX - SYMBOLS AND CALCULATIONS

A	area, sq ft
c_p	specific heat at constant pressure
d	diameter, ft
f	frequency, cps
g	acceleration due to gravity, 32.17 ft/sec^2
J	mechanical equivalent of heat, 778.2 ft-lb/Btu
N	rotor speed, rpm
$N/\sqrt{\theta}$	corrected speed, rpm
P	total pressure, lb/sq ft
R	gas constant, 53.35 ft-lb/(lb)(^{o}F)
T	stagnation temperature, ^{o}R
U	wheel speed, ft/sec
V	velocity, ft/sec
W	weight flow, lb/sec
$W_a\sqrt{\theta}/\delta$	corrected airflow, lb/sec
γ	ratio of specific heats
δ	ratio of total pressure to NACA standard sea-level pressure of 2116 lb/sq ft
η_{ad}	adiabatic efficiency
θ	ratio of total temperature to NACA standard sea-level temperature of 518.7^o R
λ	number of stall zones
φ	flow coefficient, $\left(V_x/U\right) = \frac{60R}{\pi d_m A}\frac{W_a}{N}\frac{T_I}{P_I}$

[redacted]

ψ pressure coefficient,

$$\frac{gJc_pT_{st}}{(V_m/\sqrt{\theta})^2}\left[\left(\frac{P_0}{P_I}\right)^{\frac{\gamma-1}{\gamma}} - 1\right] = \frac{3600\ gJc_pT_I}{n(\pi d_m N)^2}\left[\left(\frac{P_0}{P_I}\right)^{\frac{\gamma-1}{\gamma}} - 1\right]$$

Subscripts:

a	air
I	stage inlet
i	inner
m	mean
n	number of stages in group
0	stage outlet
o	outer
r	rated
st	standard
x	axial
1-9	stages in outer spool
10-16	stages in inner spool

Calculation of Stage Stall Line

The first step in computing the stage-stall line presented in figure 24 was the determination of the peak pressure-coefficient value for this group of stages. In figure 16 is presented the loading curve for this stage, obtained from steady-state points. However, there is not sufficient data here to be assured of the maximum pressure coefficient. To obtain the peak value, the exhaust-nozzle area was decreased until surge was obtained. Then steady-state points were taken at several speeds just prior to the point of stall. These points, at the stall loading of this outlet group of stages, clustered around a pressure coefficient value of 0.32. Using this value and the above definition of pressure coefficient, the stall pressure ratio was calculated for a range of compressor speeds.

[redacted]

REFERENCES

1. Stodola, A.: Steam and Gas Turbines. Vol. II. McGraw-Hill Book Co., Inc., 1927, pp. 1265-1666.

2. Bullock, Robert O., Wilcox, Ward W., and Moses, Jason J.: Experimental and Theoretical Studies of Surging in Continuous-Flow Compressors. NACA Rep. 861, 1946. (Supersedes NACA TN 1213.)

3. Brook, G. V.: Surging in Centrifugal Superchargers. R. & M. No. 1503, British ARC, 1933.

4. Medeiros, Arthur A., Benser, William A., and Hatch, James E.: Analysis of Off-Design Performance of a 16-Stage Axial-Flow Compressor with Various Blade Modifications. NACA RM E52L03, 1953.

5. Jackson, Robert J.: Effect on the Weight-Flow Range and Efficiency of a Typical Axial-Flow Compressor Inlet Stage That Result from the Use of a Decreased Blade Camber or Decreased Guide-Vane Turning. NACA RM E52G02, 1952.

6. Rebeske, John J., Jr., and Dugan, James F., Jr.: Acceleration of High-Pressure-Ratio Single-Spool Turbojet Engine as Determined from Component Performance Characteristics. II - Effect of Compressor Interstage Air Bleed. NACA RM E53E06, 1953.

7. Budinger, Ray E., and Kaufman, Harold R.: Investigation of the Performance of a Turbojet Engine with Variable-Position Compressor Inlet Guide Vanes. NACA RM E54L23a, 1955.

8. Wallner, Lewis E., and Lubick, Robert J.: Steady-State and Surge Characteristics of a Compressor Equipped with Variable Inlet Guide Vanes Operating in a Turbojet Engine. NACA RM E54I28, 1955.

9. Mallett, William E., and Groesbeck, Donald E.: Effects of Compressor Interstage Bleed and Adjustable Inlet Guide Vanes on Compressor Stall Characteristics of a High-Pressure-Ratio Turbojet Engine at Altitude. NACA RM E55G27, 1955.

10. Fenn, David B., and Sivo, Joseph N.: Effect of Inlet Flow Distortion on Compressor Stall and Acceleration Characteristics of a J65-B-3 Turbojet Engine. NACA RM E55F20, 1955.

11. Smith, A. G., and Fletcher, P. J.: Observations on the Surging of Various Low-Speed Fans and Compressors. Memo. No. M.219, British NGTE, July 1954.

[redacted]

12. Grant, Howard P.: Hot Wire Measurements of Stall Propagation and Pulsating Flow in an Axial Flow Inducer-Centrifugal Impeller System. Pratt and Whitney Res. Rep. No. 133, June 1951.

13. Huppert, Merle C.: Preliminary Investigation of Flow Fluctuations During Surge and Blade Row Stall in Axial-Flow Compressors. NACA RM E52E28, 1952.

14. Iura, T., and Rannie, W. D.: Observations of Propagating Stall in Axial-Flow Compressors. Rep. No. 4, Mech. Eng. Lab., C.I.T., Apr. 1953. (Navy Contract N6-ORI-102, Task Order 4.)

15. Huppert, Merle C., Johnson, Donald F., and Costilow, Eleanor L.: Preliminary Investigation of Compressor Blade Vibration Exited by Rotating Stall. NACA RM E52J15, 1952.

16. Wallner, Lewis E., Lubick, Robert J., and Bloomer, Harry E.: Evaluation of an Automatic Inlet-Pressure Control Valve for Study of Transient Engine Performance Characteristics. NACA RM E55L13, 1956.

17. Dugan, James F., Jr.: Two-Spool Matching Procedures and Equilibrium Characteristics of a Two-Spool Turbojet Engine. NACA RM E54F09, 1954.

18. Huppert, Merle C., and Benser, William A.: Some Stall and Surge Phenomena in Axial-Flow Compressors. Jour. Aero. Sci., vol. 20, no. 12, Dec. 1953, pp. 835-845.

[redacted]

TABLE I. - INSTRUMENTATION

Station	Steady state			Transient	
	Number of total-pressure probes	Number of static-pressure probes	Number of thermocouple probes	Number of total-pressure probes	
				Fixed	Variable
0	42	16	16	1	-
1	15	2	15	1	4
3	12	--	12	1	-
6	12	--	12	1	-
9	24	--	12	1	4
10	9	--	9	1	-
13	9	--	9	1	4
16	20	--	12	1	-

[redacted]

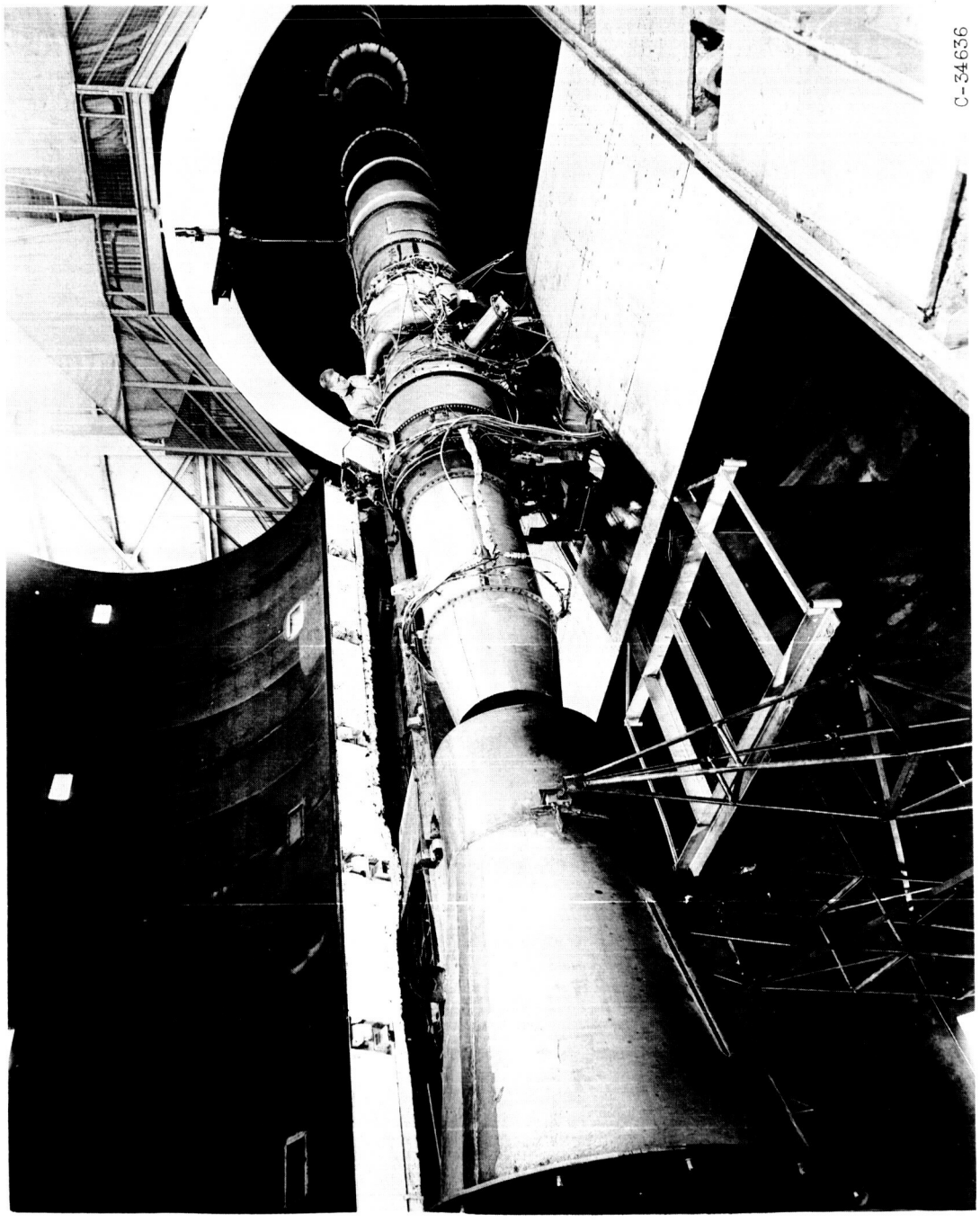

C-34636

Figure 1. - Two-spool turbojet engine installed in altitude wind tunnel.

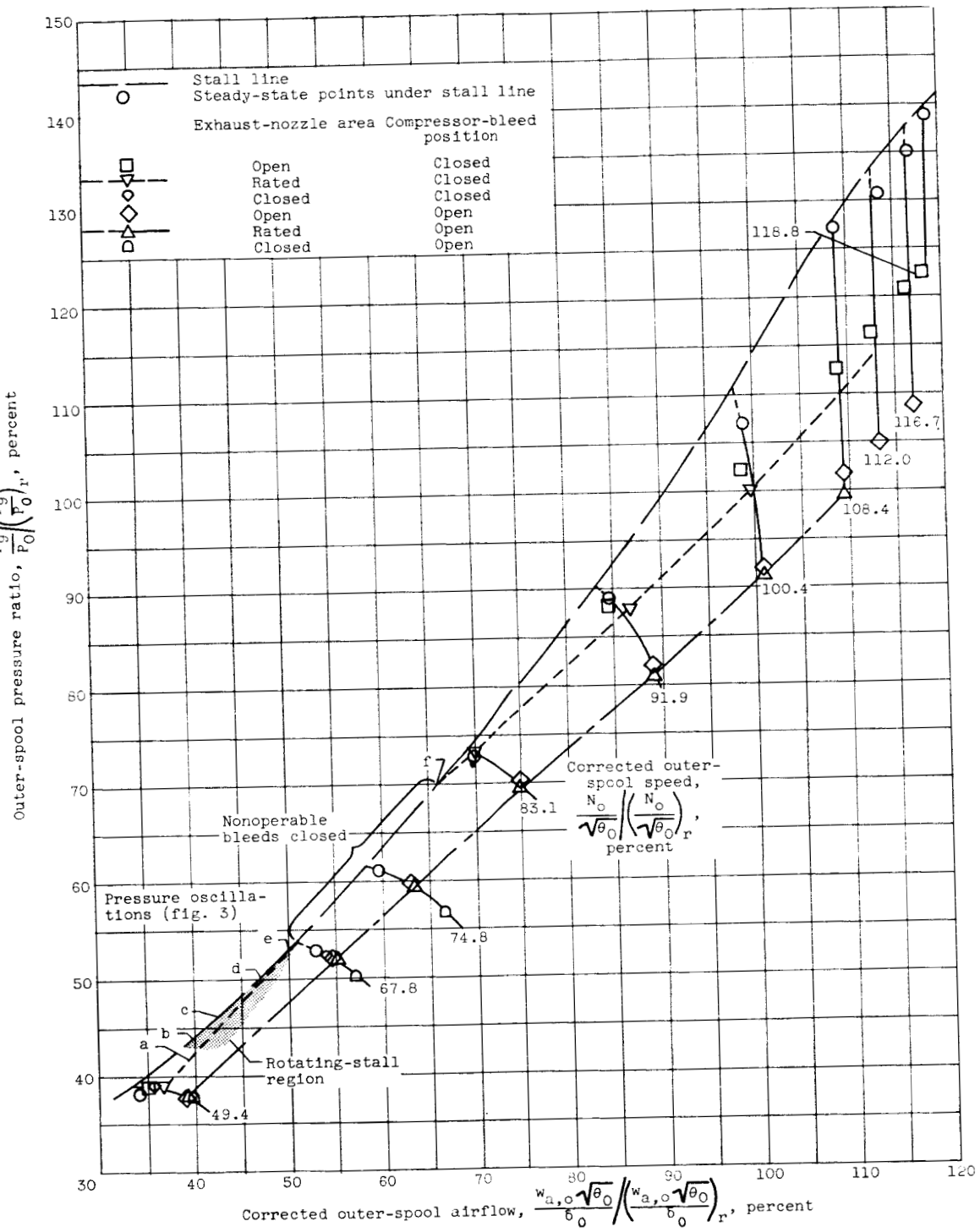

Figure 2. - Over-all performance of outer spool. Altitude, 35,000 feet; flight Mach number, 0.8.

[redacted]

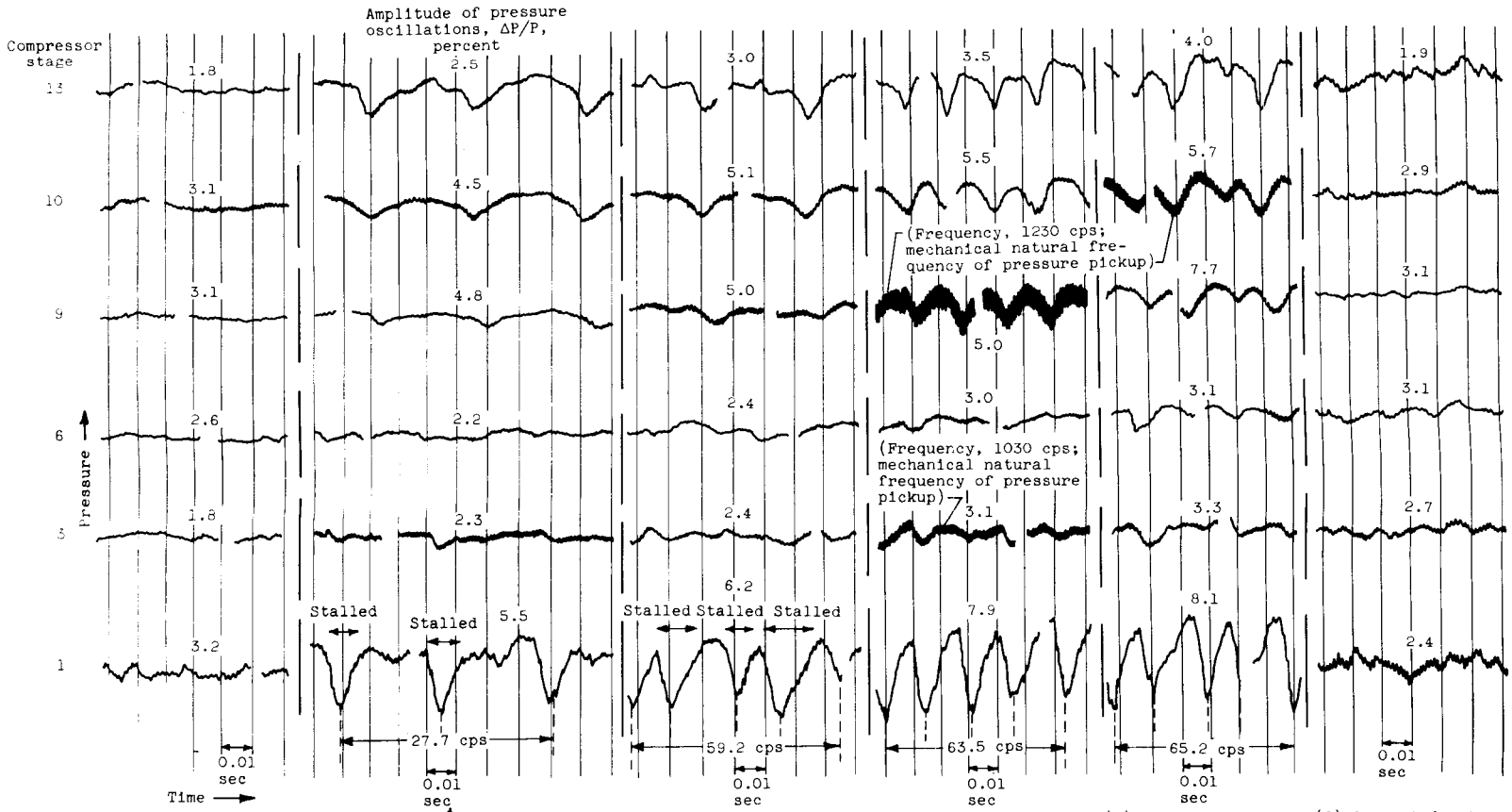

(a) Corrected outer-spool speed $\frac{N_o}{\sqrt{\theta_o}} \Big/ \left(\frac{N_o}{\sqrt{\theta_o}}\right)_r$, 55.2 percent; rotating-stall zone λ, 0.

(b) Corrected outer-spool speed $\frac{N_o}{\sqrt{\theta_o}} \Big/ \left(\frac{N_o}{\sqrt{\theta_o}}\right)_r$, 57.0 percent; rotating-stall zone λ, 1.

(c) Corrected outer-spool speed $\frac{N_o}{\sqrt{\theta_o}} \Big/ \left(\frac{N_o}{\sqrt{\theta_o}}\right)_r$, 61.0 percent; rotating-stall zone λ, 2.

(d) Corrected outer-spool speed $\frac{N_o}{\sqrt{\theta_o}} \Big/ \left(\frac{N_o}{\sqrt{\theta_o}}\right)_r$, 65.2 percent; rotating-stall zone λ, 2.

(e) Corrected outer-spool speed $\frac{N_o}{\sqrt{\theta_o}} \Big/ \left(\frac{N_o}{\sqrt{\theta_o}}\right)_r$, 67.3 percent; rotating-stall zone λ, 2.

(f) Corrected outer-spool speed $\frac{N_o}{\sqrt{\theta_o}} \Big/ \left(\frac{N_o}{\sqrt{\theta_o}}\right)_r$, 78.4 percent; rotating-stall zone λ, 0.

Figure 3. - Interstage pressure traces plotted at varying speeds. Compressor bleeds closed; altitude, 35,000 feet.

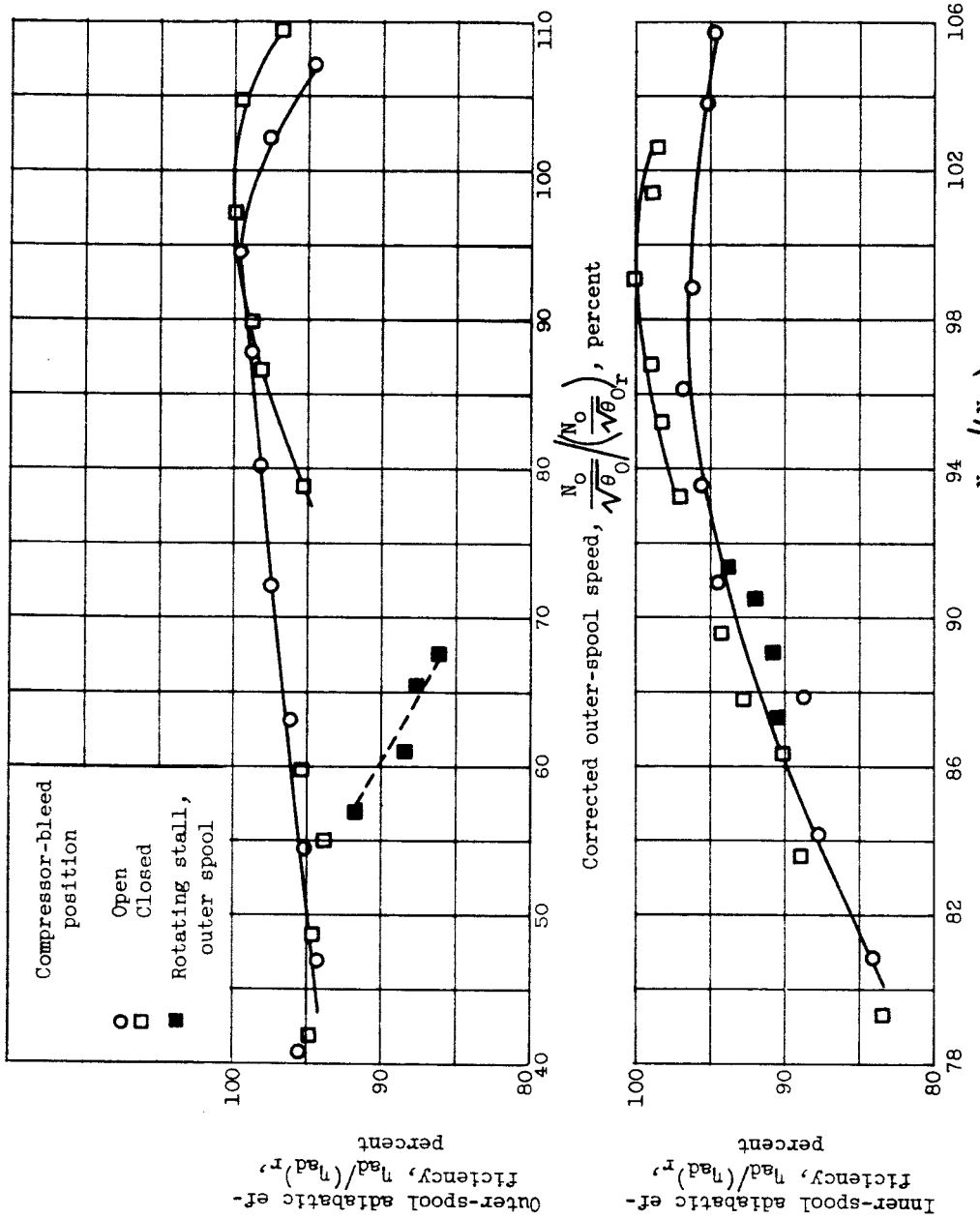

Figure 4. - Effect of rotor speed on compressor efficiency. Altitude, 35,000 feet; flight Mach number, 0.8; rated exhaust-nozzle area.

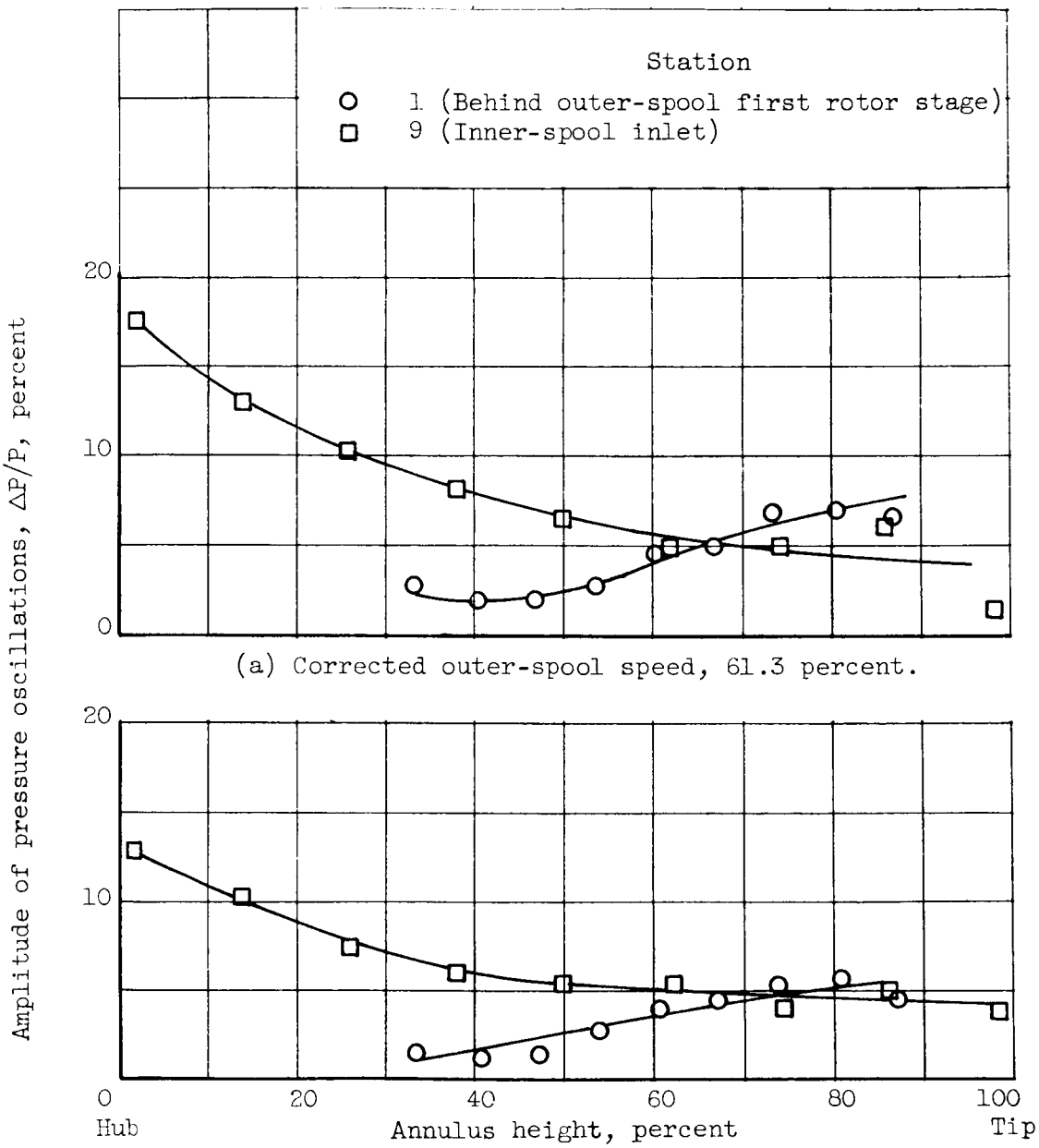

(a) Corrected outer-spool speed, 61.3 percent.

(b) Corrected outer-spool speed, 56.0 percent.

Figure 5. - Variation of rotating-stall pressure amplitude with radial position. Altitude, 35,000 feet; flight Mach number, 0.8; compressor bleeds closed.

[redacted]

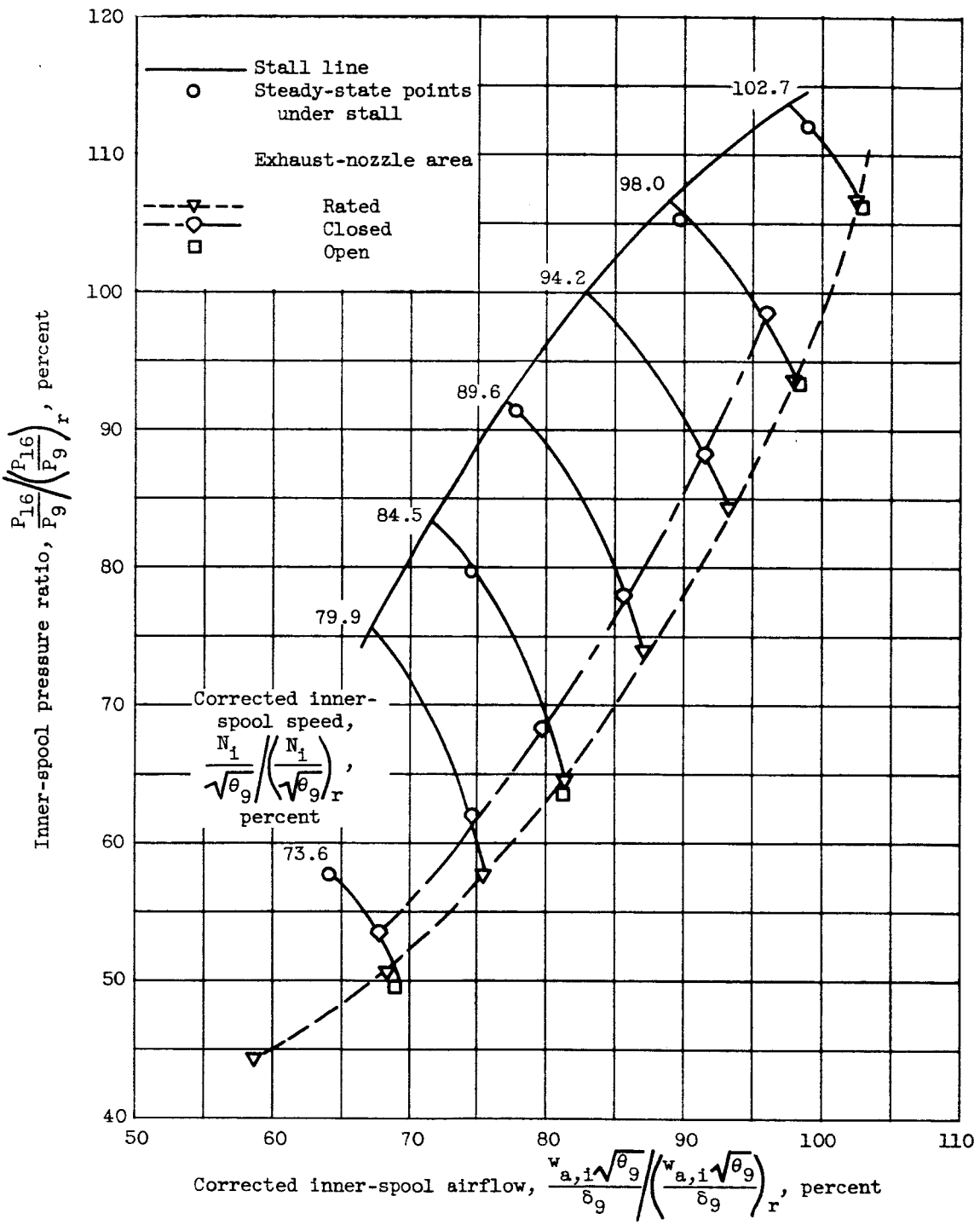

Figure 6. - Over-all performance of inner spool. Altitude, 35,000 feet; flight Mach number, 0.8; compressor bleeds closed.

[redacted]

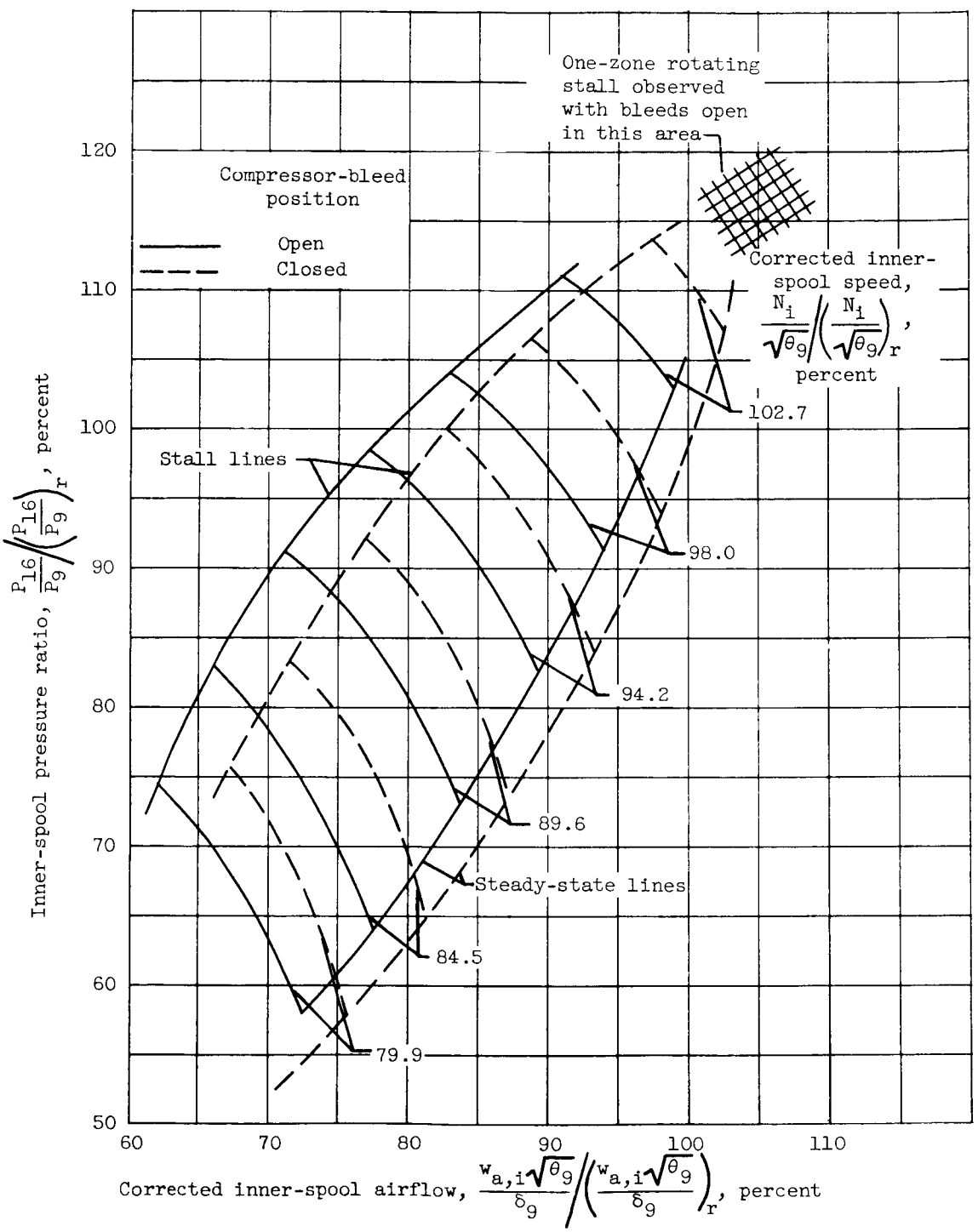

Figure 7. - Effect of intercompressor bleed on inner-spool map. Altitude, 35,000 feet; flight Mach number, 0.8; rated exhaust-nozzle area.

[redacted]

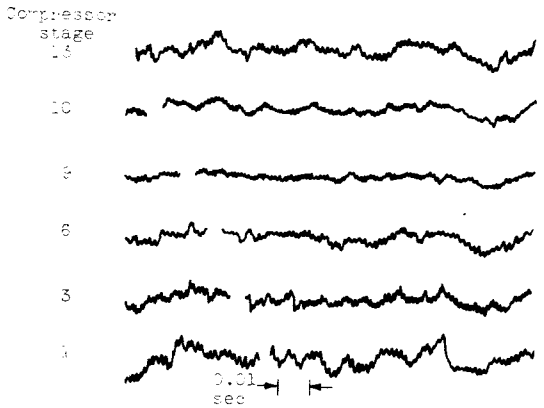

(a) No rotating stall observed at corrected inner-spool speeds $\frac{N_i}{\sqrt{\theta_9}}\Big/\left(\frac{N_i}{\sqrt{\theta_9}}\right)_r$ as high as 103 percent.

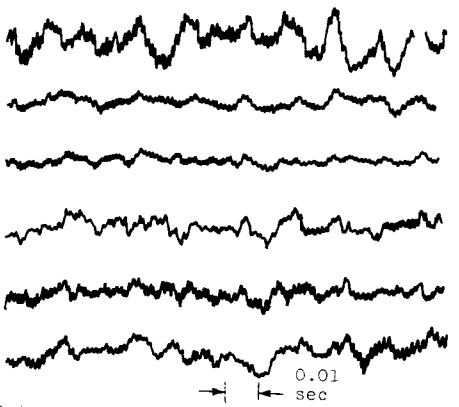

(b) Intermittent rotating stall can be seen in stage 13. Corrected inner-spool speed $\frac{N_i}{\sqrt{\theta_9}}\Big/\left(\frac{N_i}{\sqrt{\theta_9}}\right)_r$, 105 percent.

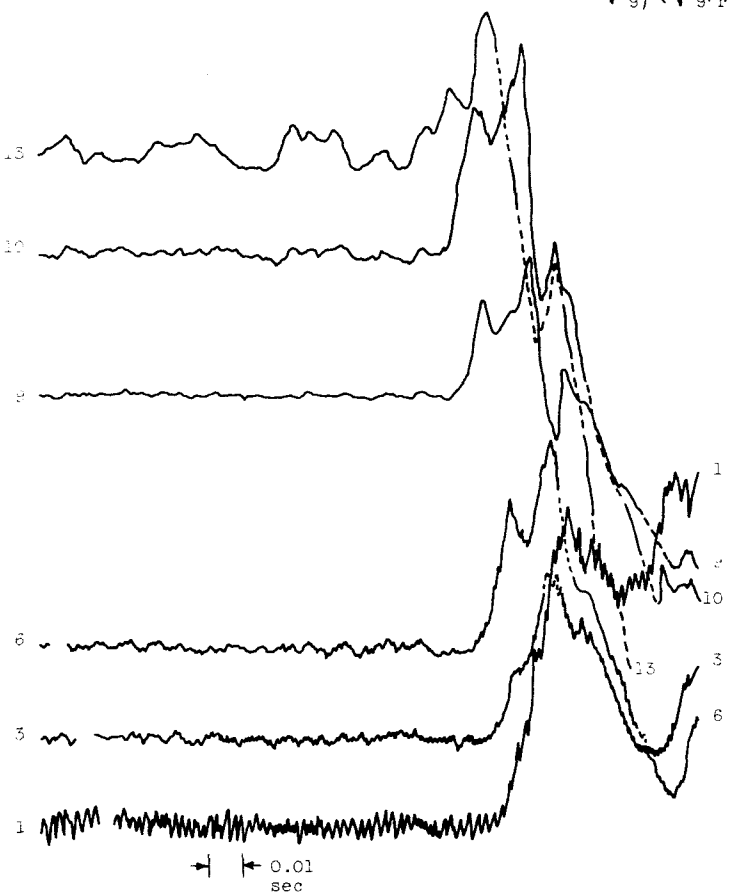

(c) Intermittent rotating stall into surge, visible earliest in stage 13. Corrected inner-spool speed $\frac{N_i}{\sqrt{\theta_9}}\Big/\left(\frac{N_i}{\sqrt{\theta_9}}\right)_r$, about 106.5 percent.

Figure 8. - High-speed stall inception in inner spool with compressor bleeds open.

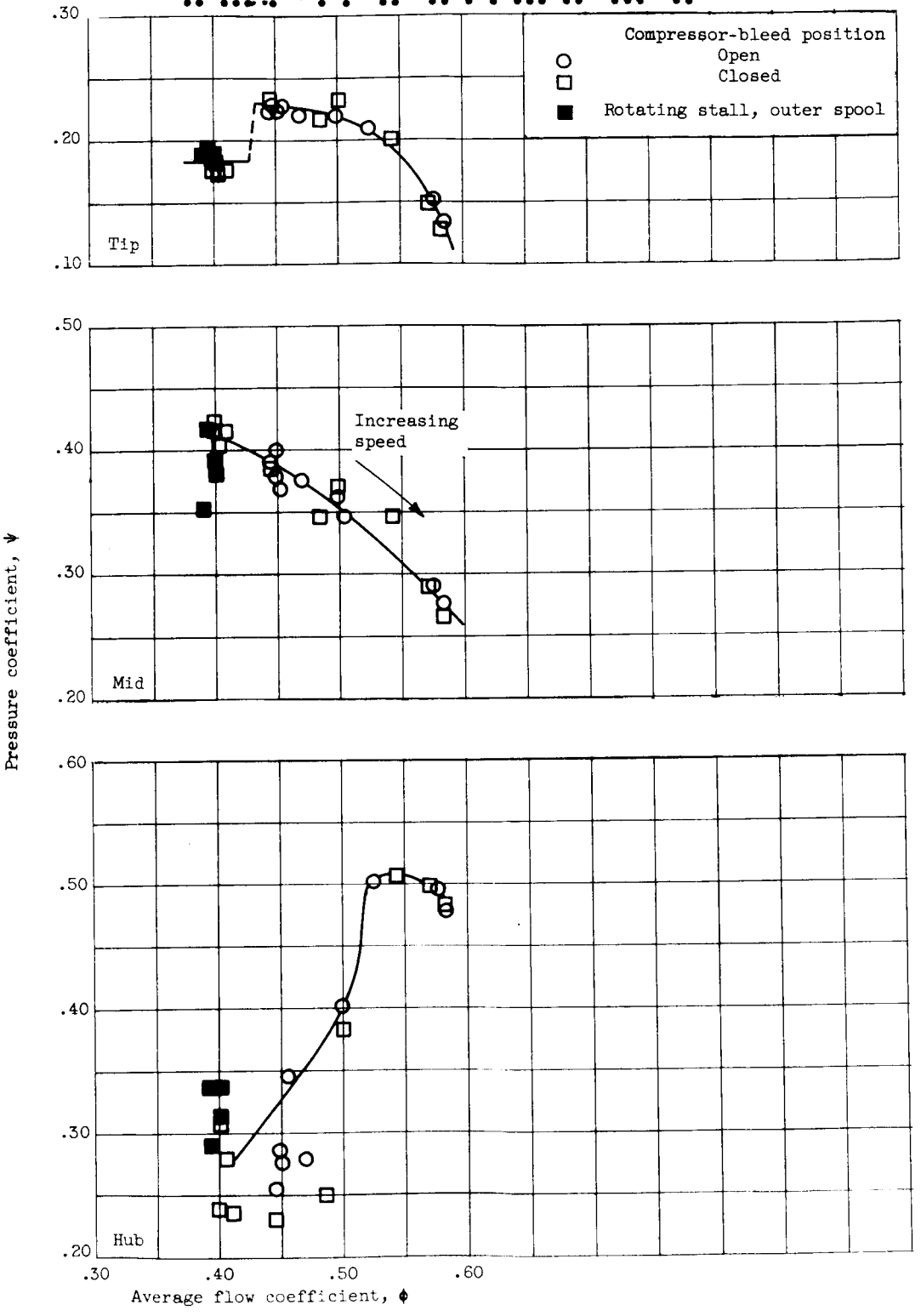

(a) Stage-loading curve.

Figure 9. - Compressor stage 1.

[redacted]

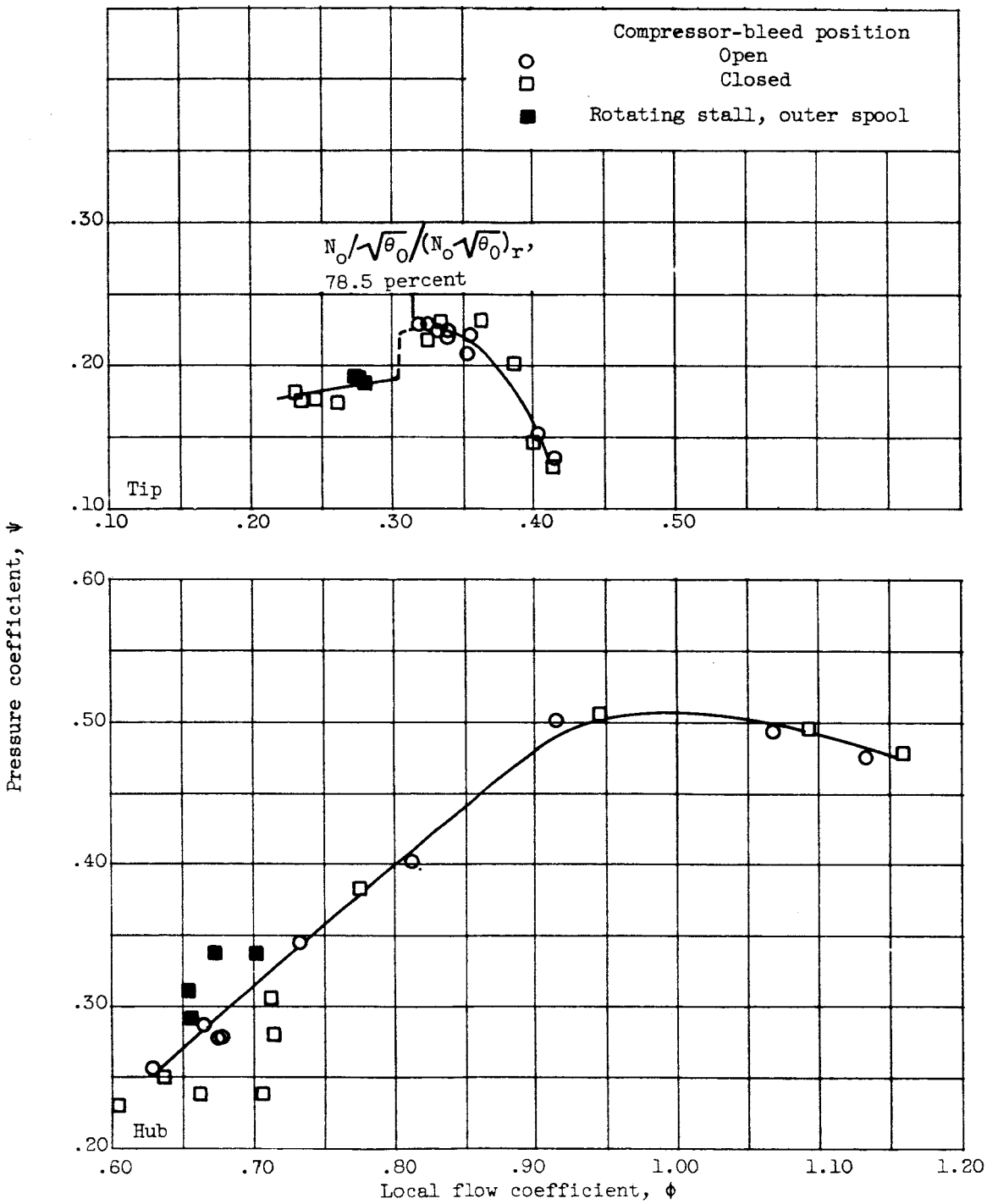

(b) Variation of pressure coefficient with local flow coefficient.

Figure 9. - Continued. Compressor stage 1.

[redacted]

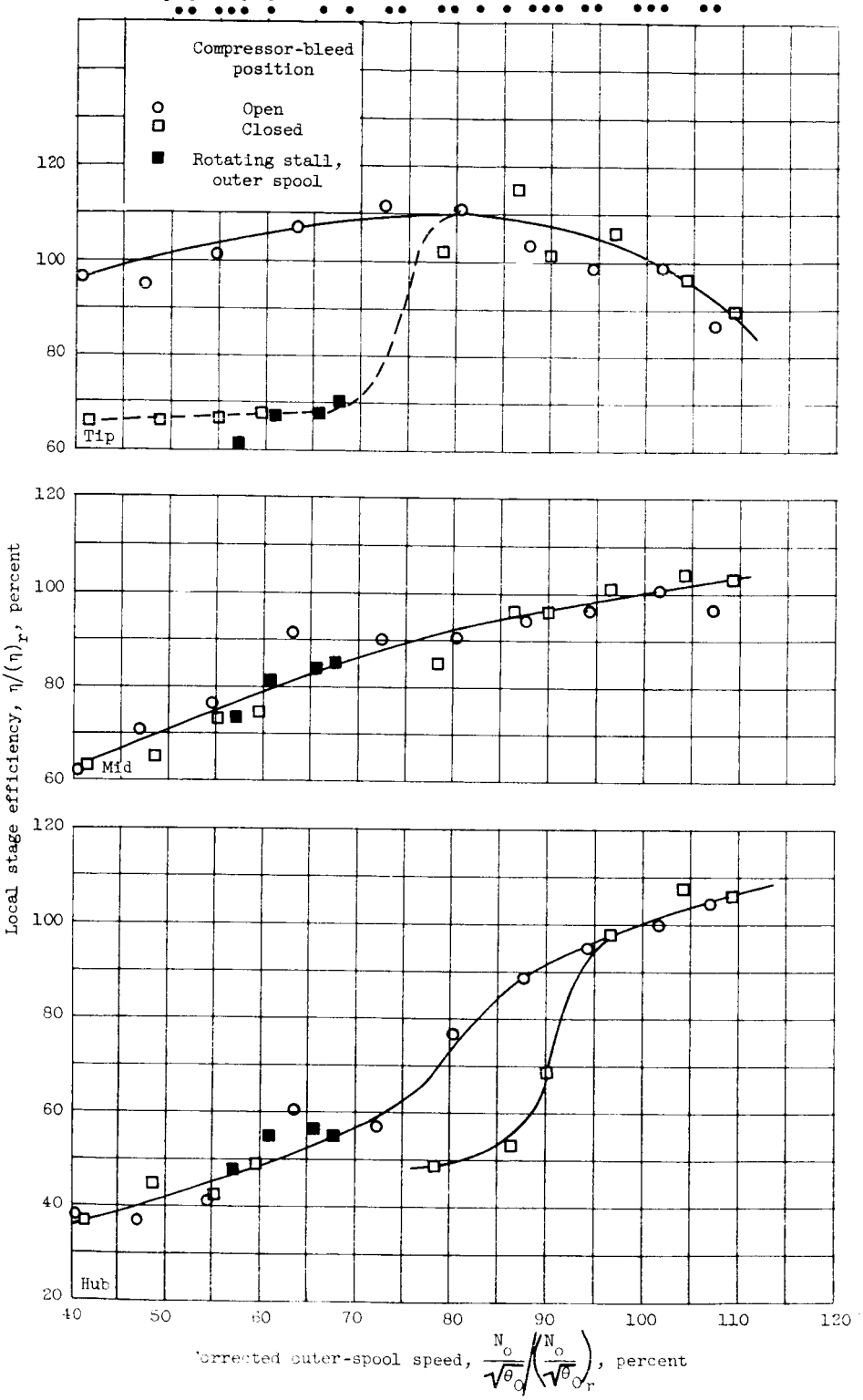

(c) Variation of local stage efficiency with outer-spool speed.

Figure 9. - Concluded. Compressor stage 1.

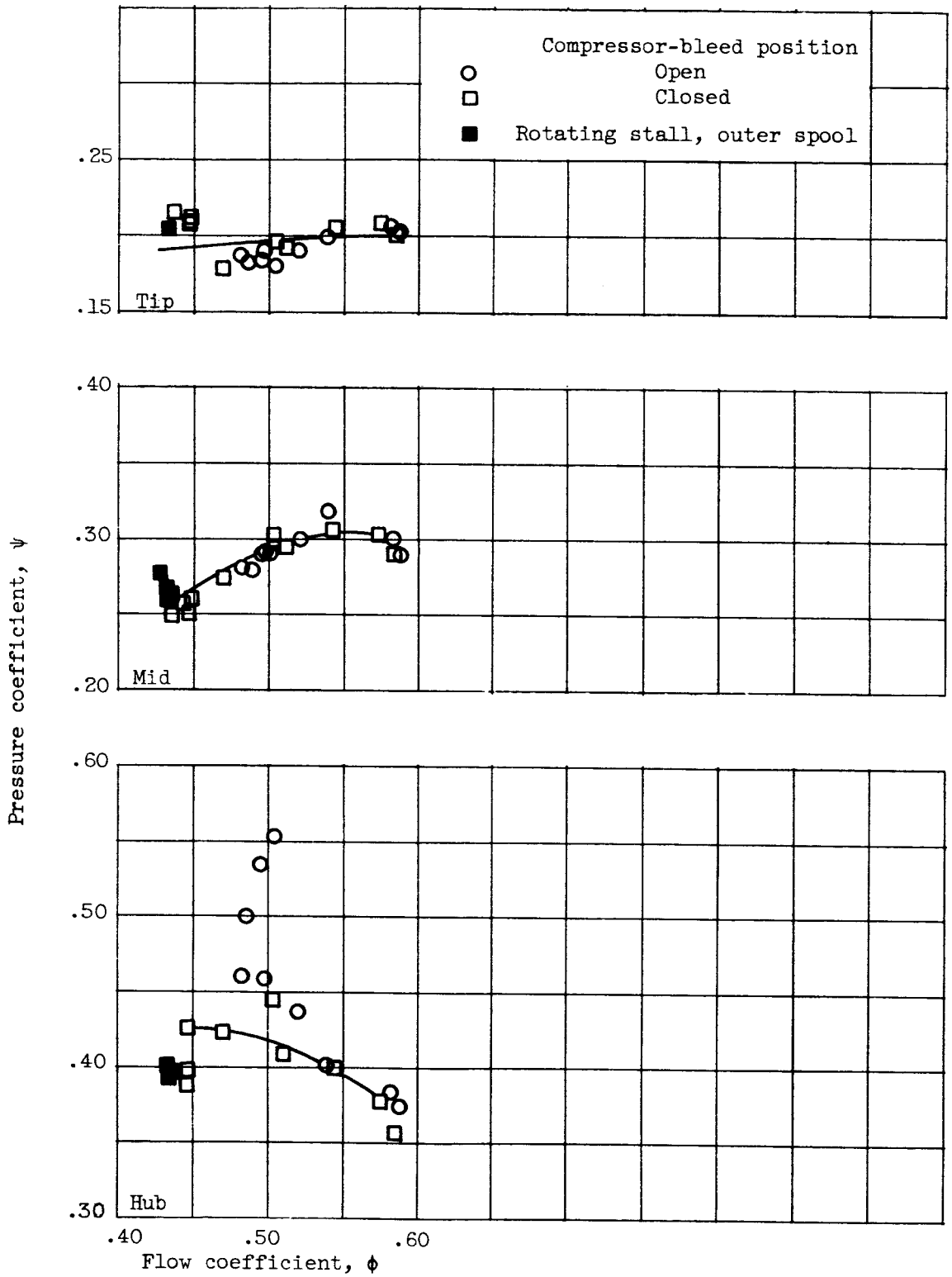

Figure 10. - Stage-loading curve for compressor stages 2 and 3.

[redacted]

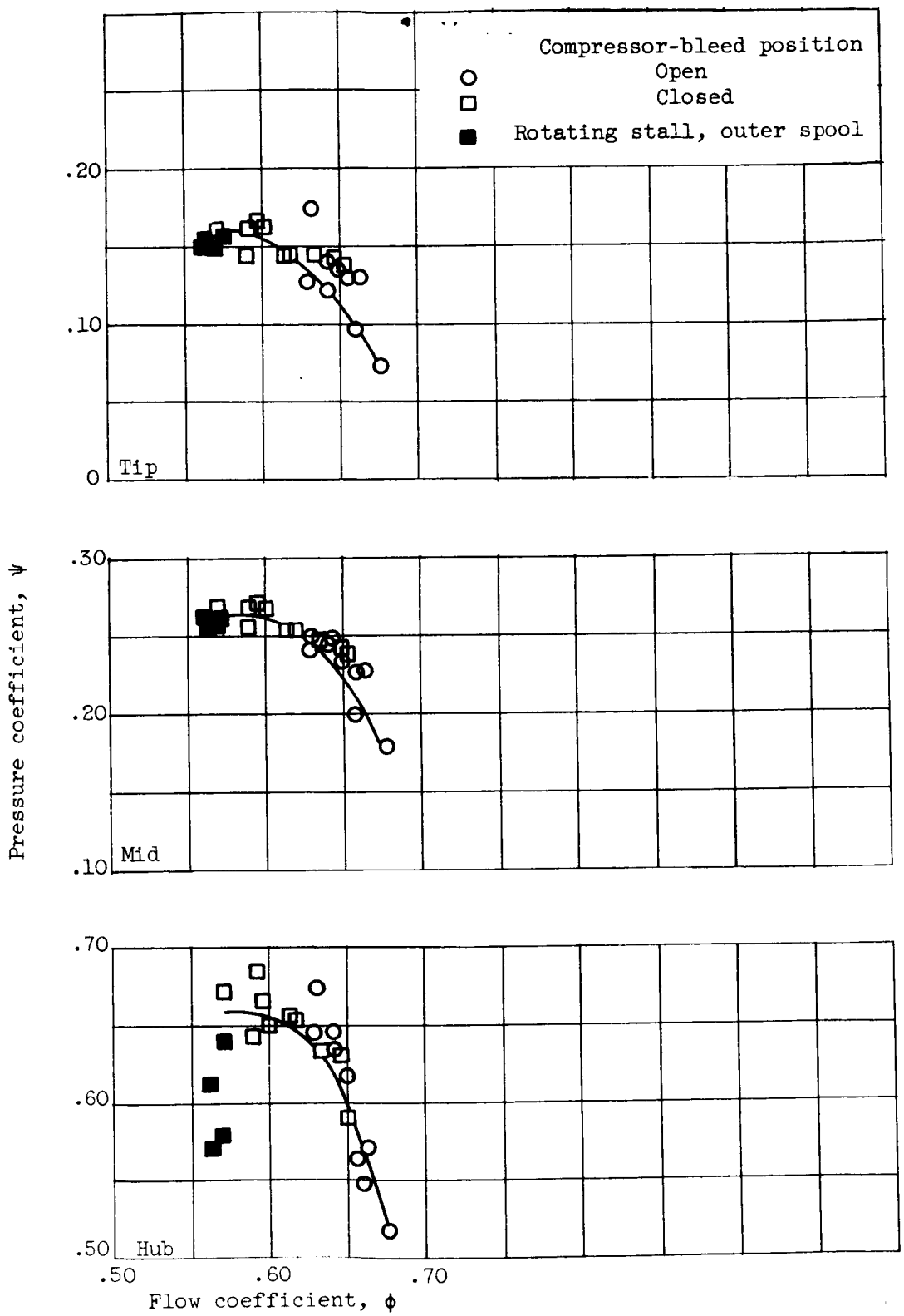

Figure 11. - Stage-loading curve for compressor stages 4 to 6.

[redacted]

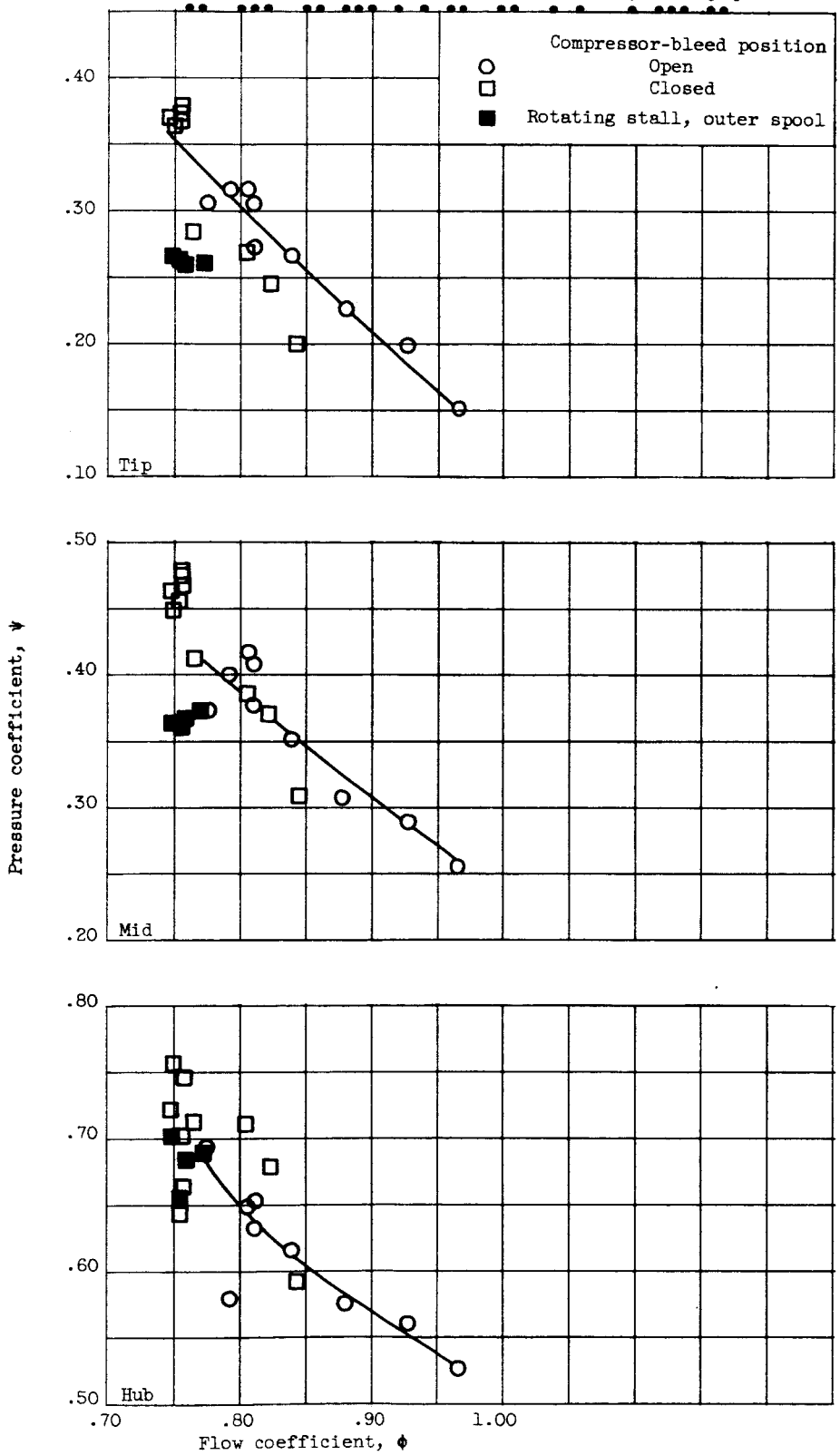

Figure 12. - Stage-loading curve for compressor stages 7 to 9.

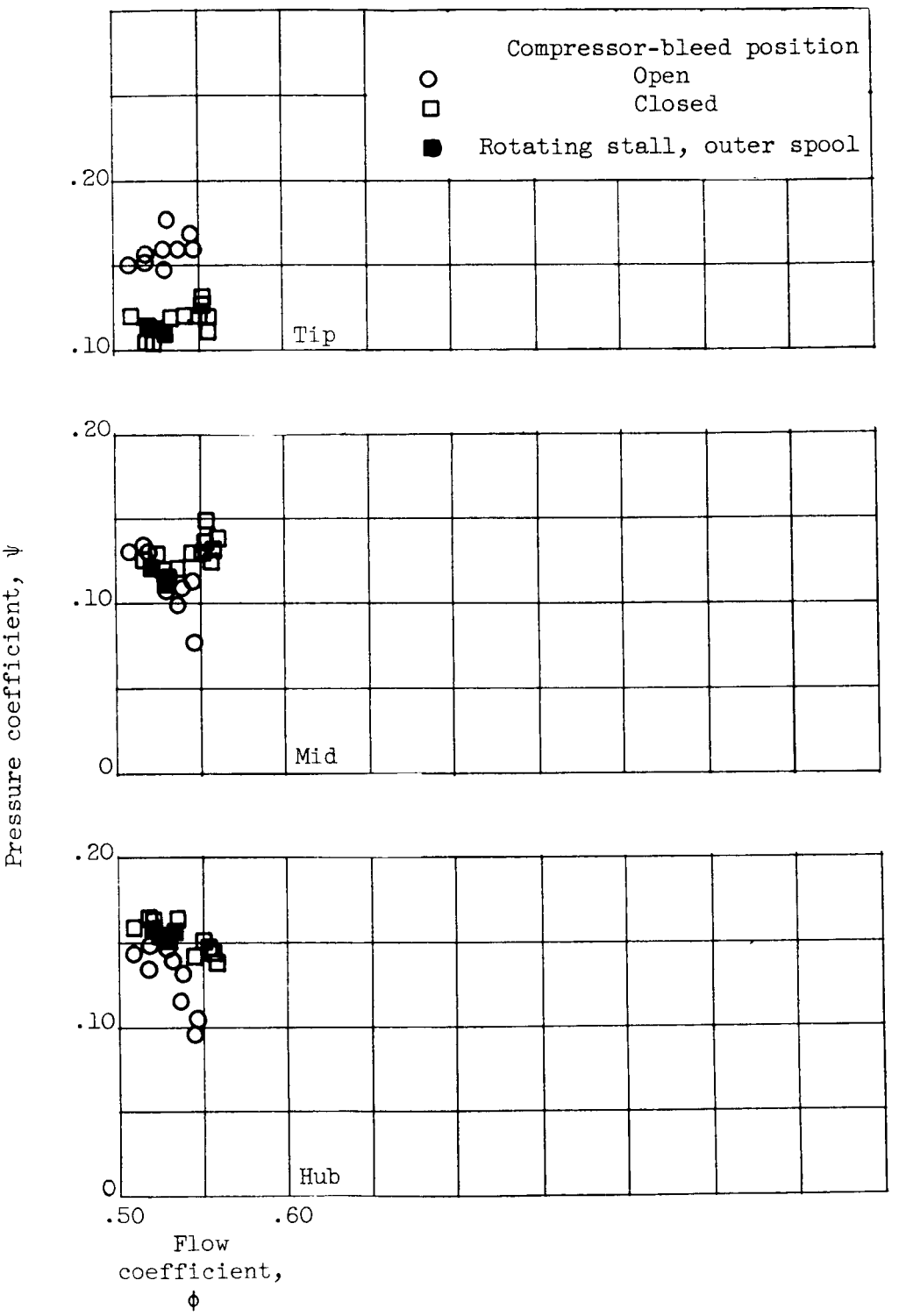

Figure 13. - Stage-loading curve for compressor stage 10. Includes losses in inter-spool transition section.

[redacted]

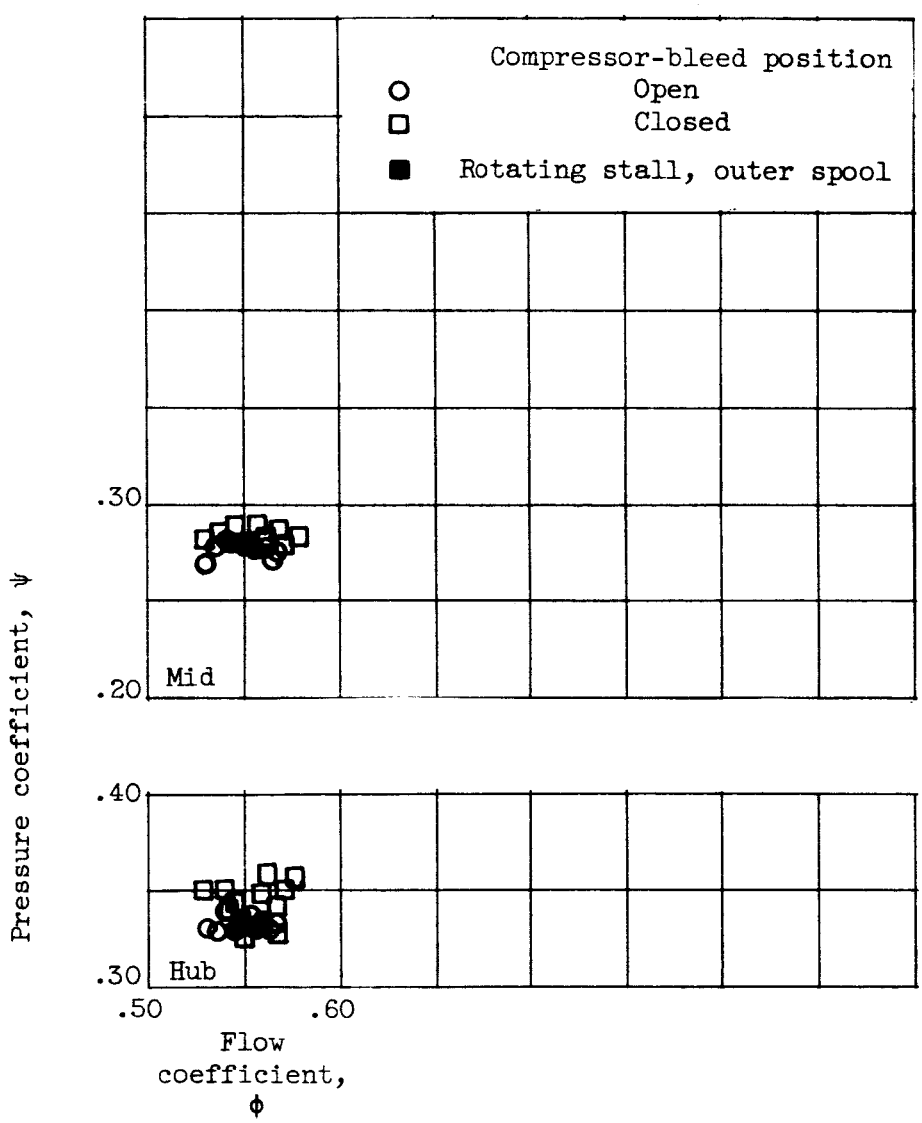

Figure 14. - Stage-loading curve for compressor stages 11 to 13.

[redacted]

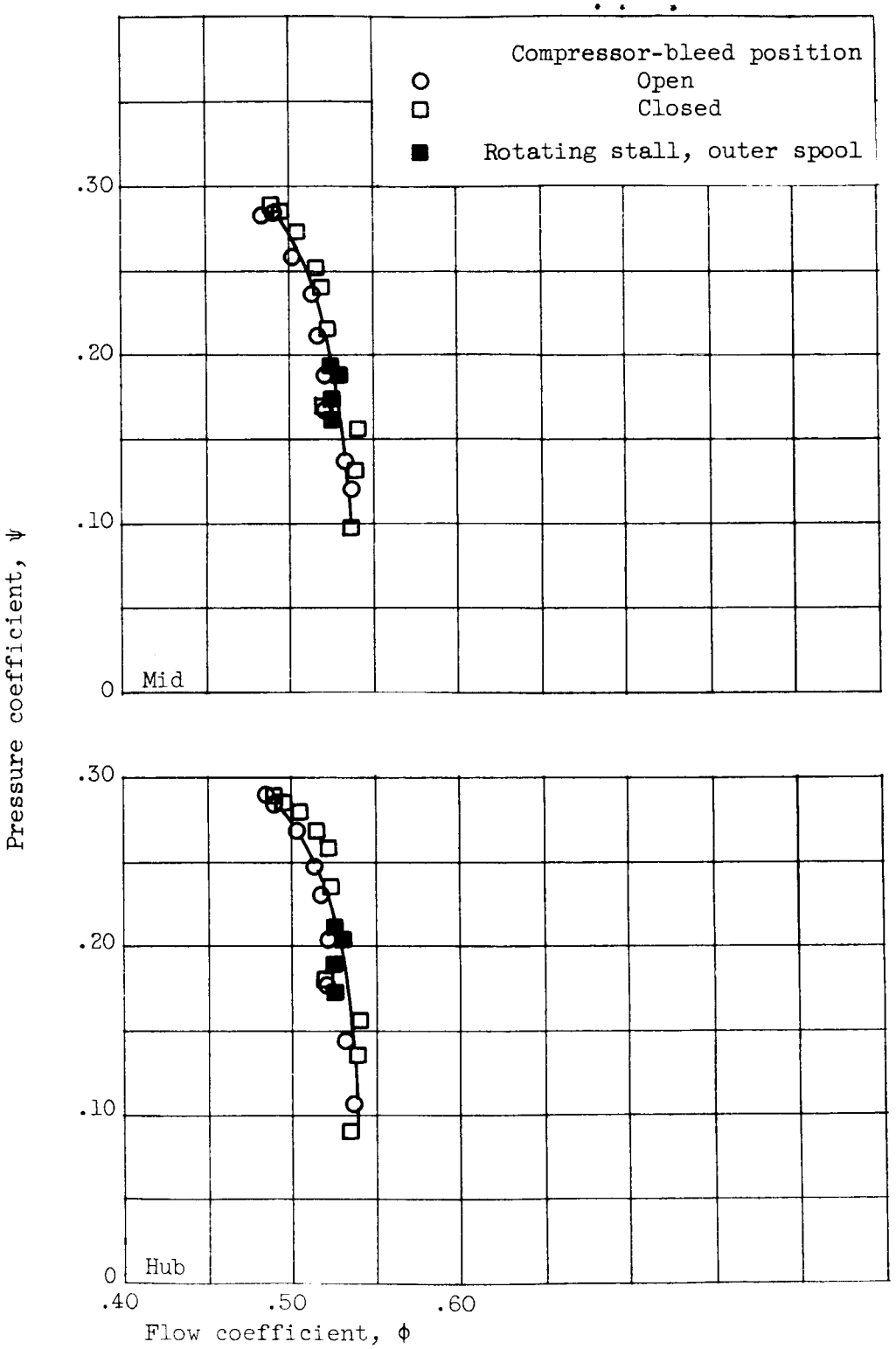

Figure 15. - Stage-loading curve for compressor stages 14 to 16.

[redacted]

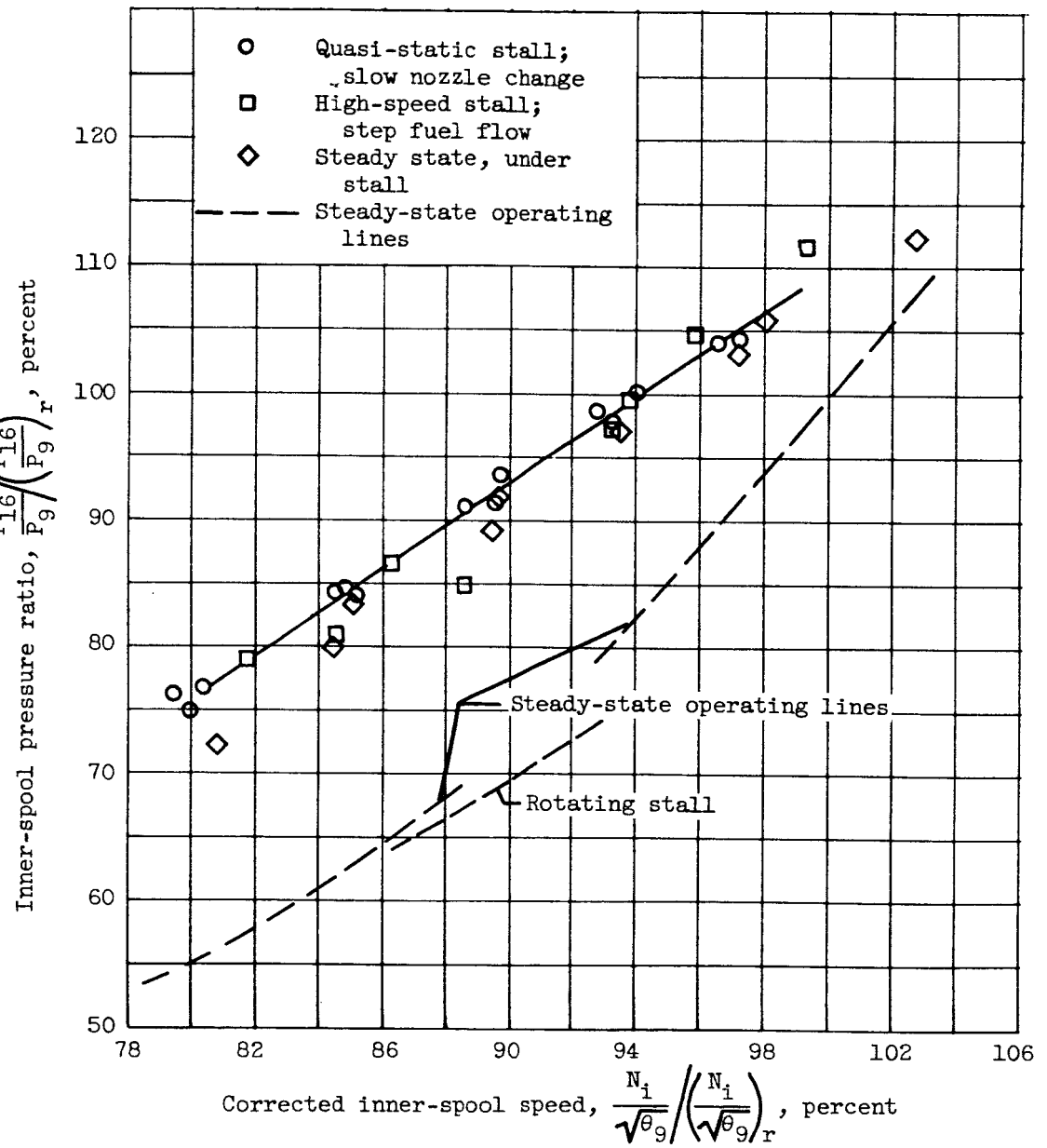

Figure 16. - Effect of approach rate on inner-spool-surge pressure ratios. Altitude, 35,000 feet; compressor bleeds closed.

[redacted]

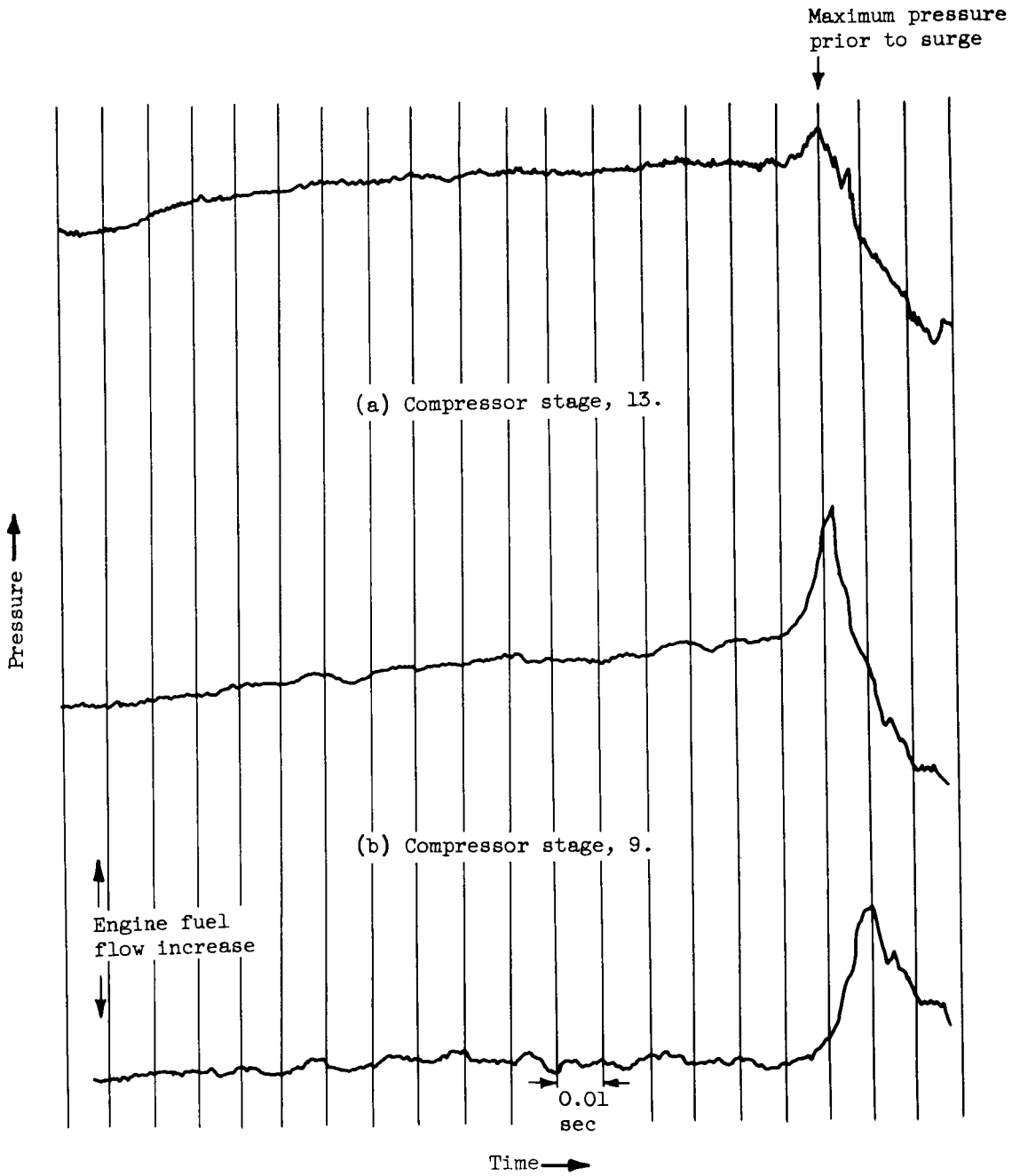

Figure 17. - Interstage pressure traces during acceleration to surge. Altitude, 35,000 feet; flight Mach number, 0.8; initial corrected outer-spool speed, 70.1 percent; initial corrected inner-spool speed, 93.2 percent.

[redacted]

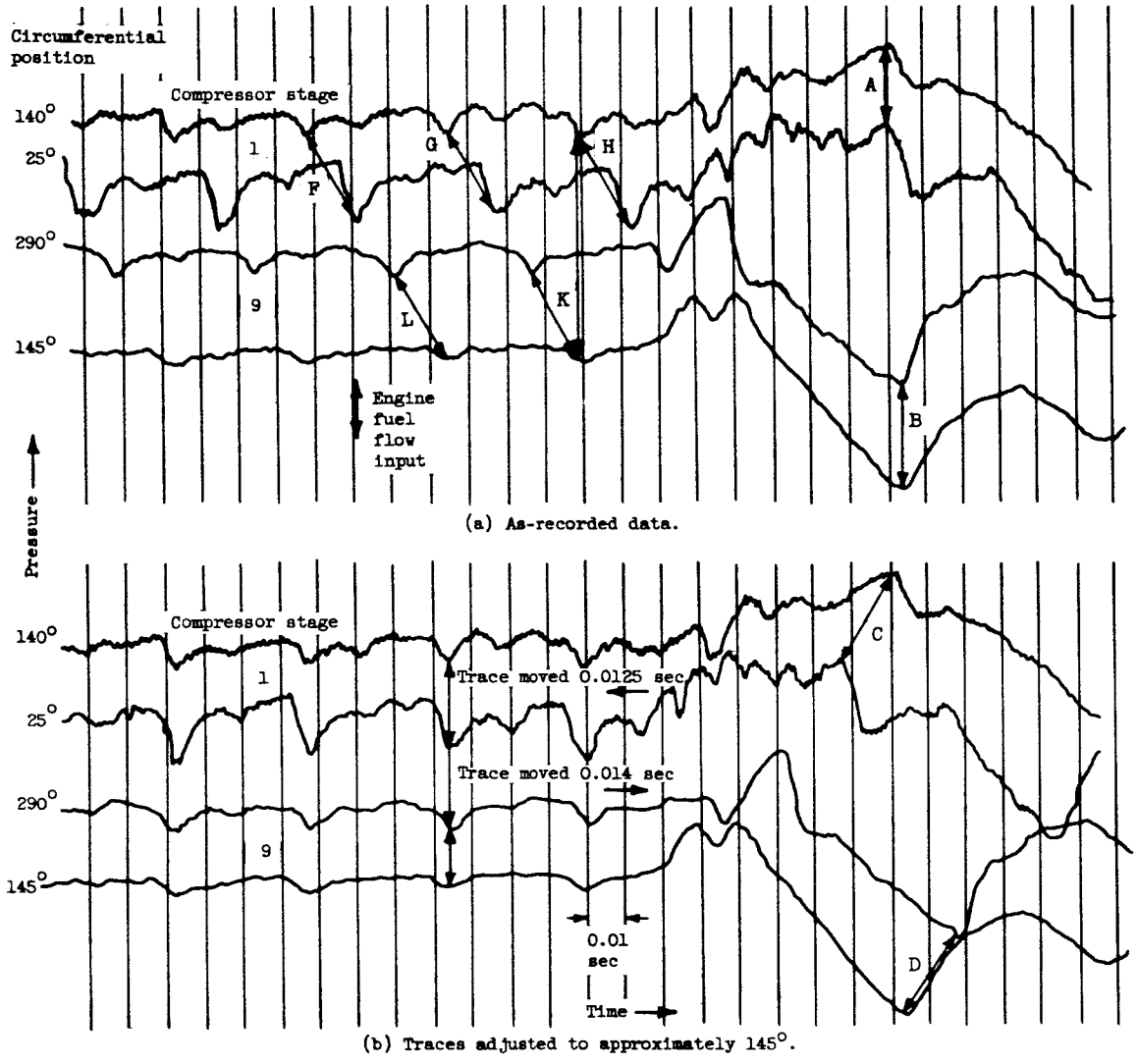

Figure 18. - Effect of circumferential position or stage pressure trace during acceleration to surge with rotating stall. Single stall segment; frequency, 27.7 cycles per second; altitude, 35,000 feet; flight Mach number, 0.8; compressor bleeds, closed. Initial conditions: corrected outer-spool speed, 57.3 percent; corrected inner-spool speed, 87.7 percent.

[redacted]

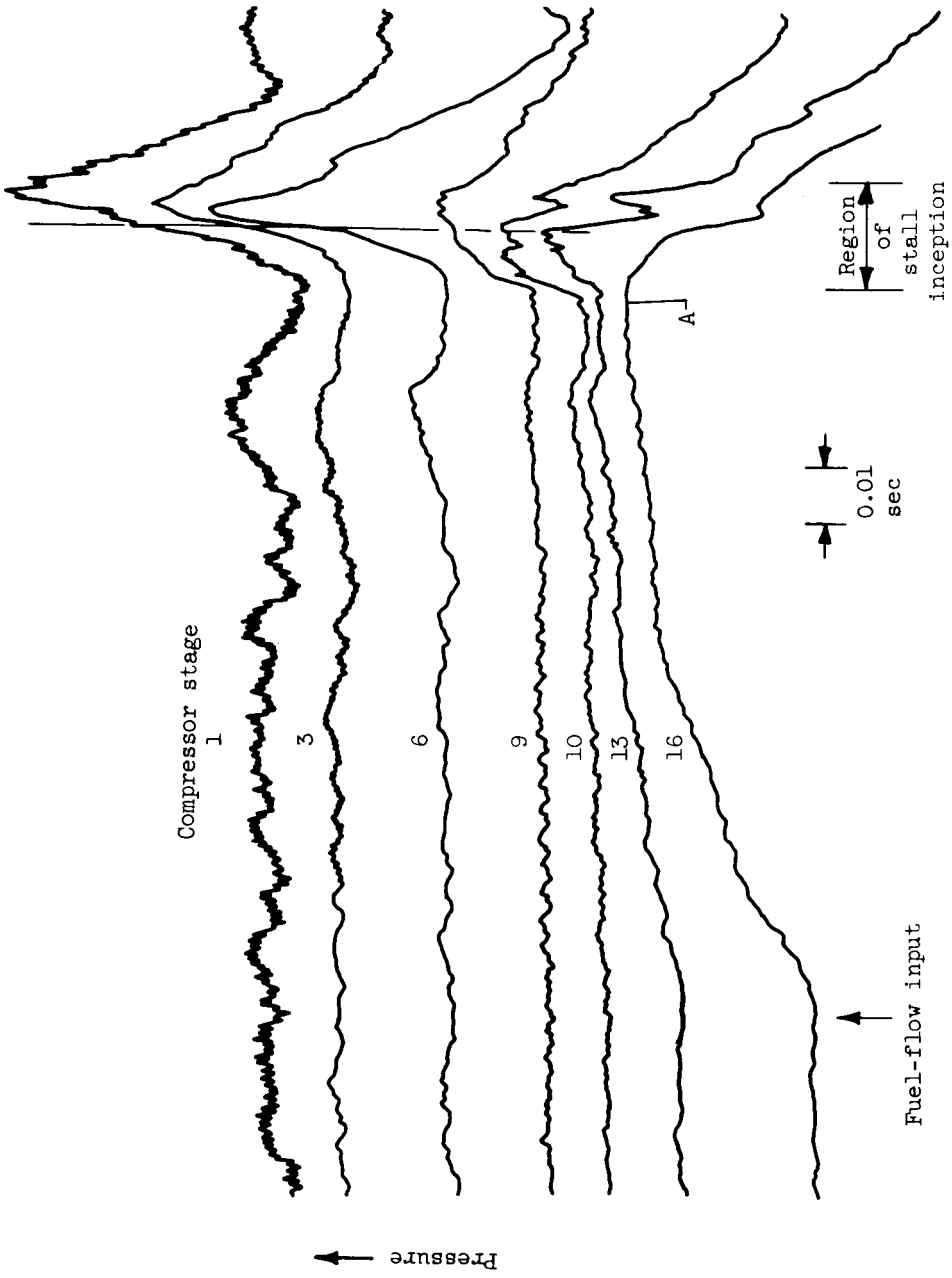

(a) Compressor bleeds open; initial corrected outer-spool speed, 58.2 percent; initial corrected inner-spool speed, 89.8 percent.

Figure 19. - Oscillograph record of interstage pressures during acceleration to surge. Altitude, 35,000 feet; flight Mach number, 0.8.

[redacted]

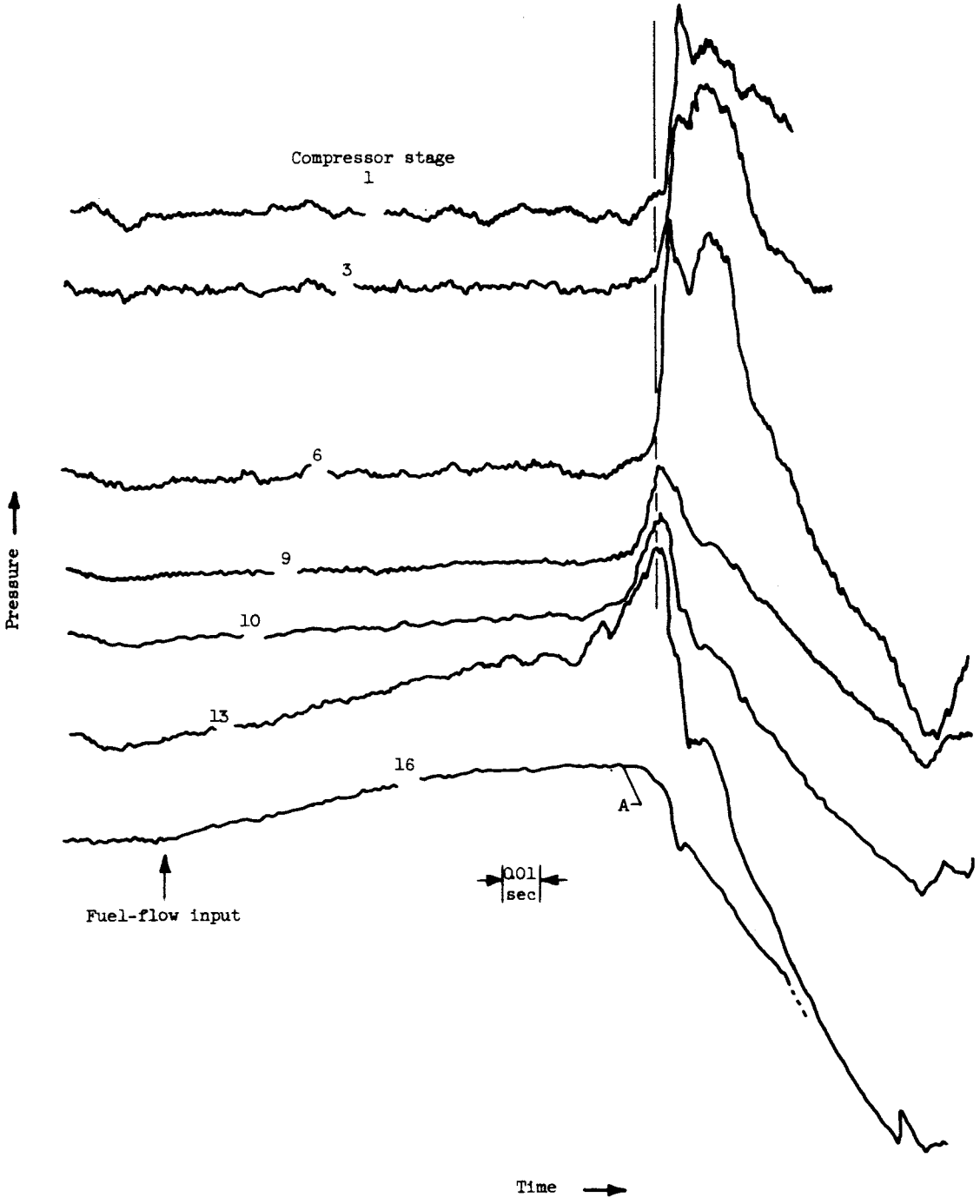

(b) Compressor bleeds closed; initial corrected outer-spool speed, 95.8 percent; initial corrected inner-spool speed, 98.9 percent.

Figure 19. - Concluded. Oscillograph record of interstage pressures during acceleration to surge. Altitude, 35,000 feet; flight Mach number, 0.8.

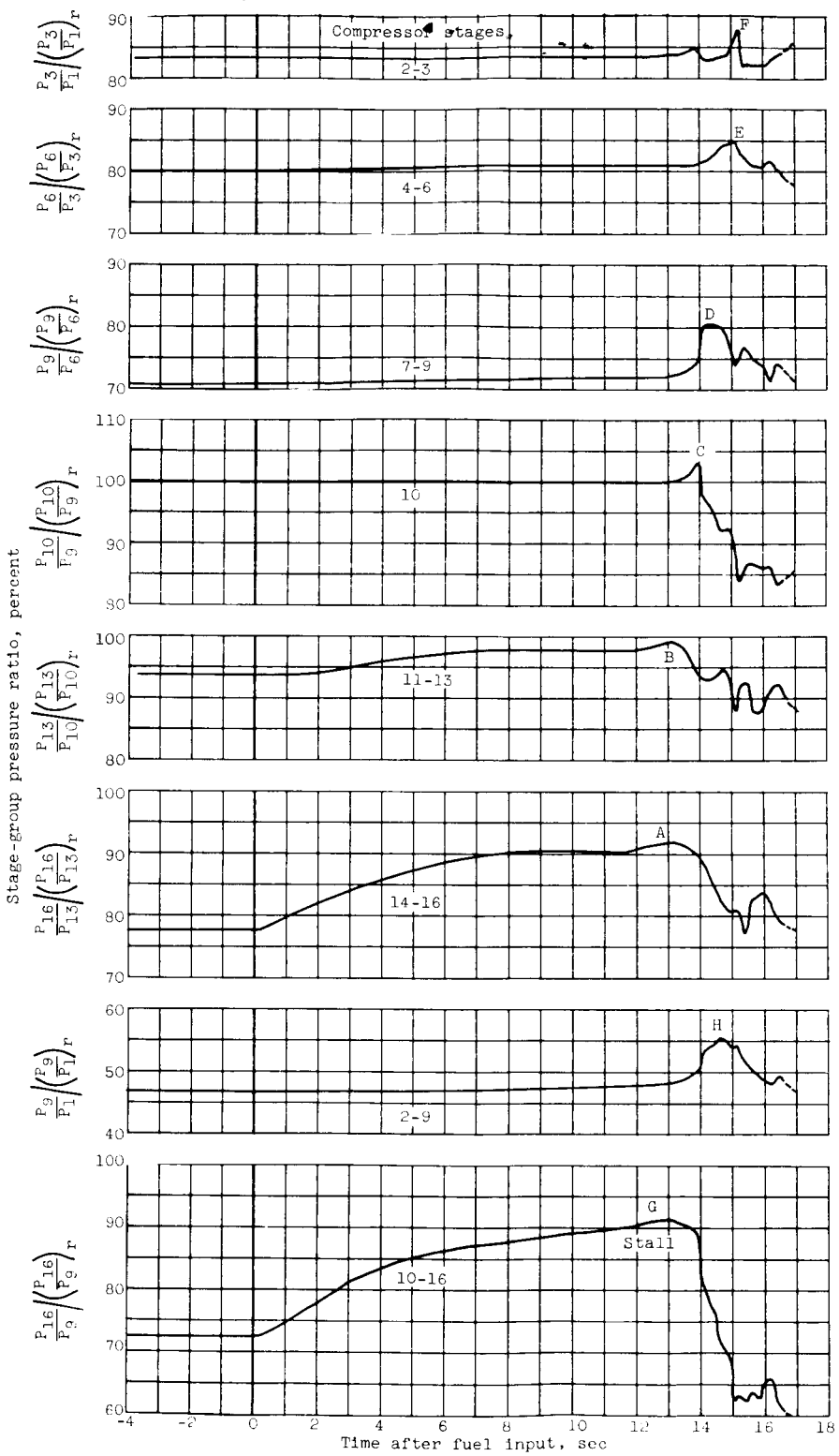

(a) Compressor bleeds open.

Figure 20. - Stage-group pressure ratio histories during acceleration to surge. Altitude, 35,000 feet; flight Mach number, 0.8.

[redacted]

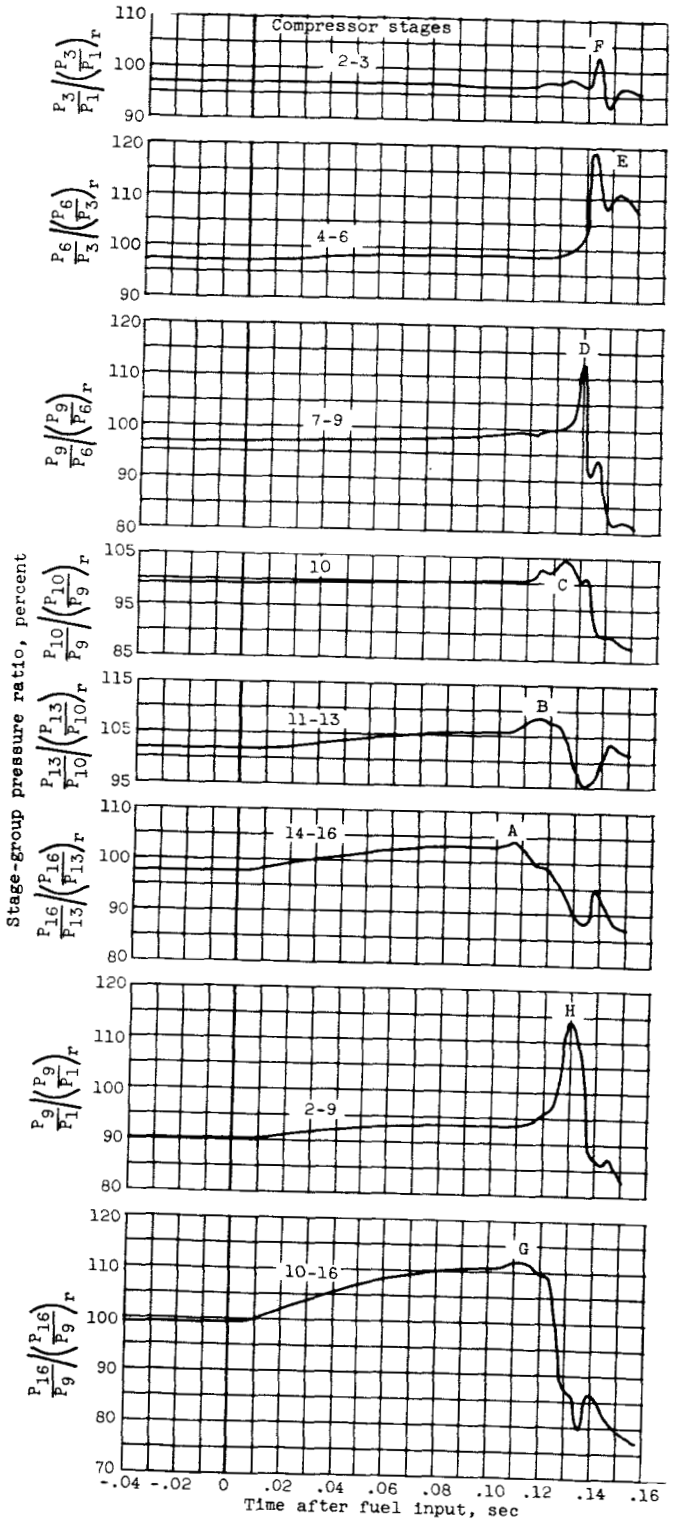

(b) Compressor bleeds closed.

Figure 20. - Concluded. Stage-group pressure ratio histories during acceleration to surge. Altitude, 35,000 feet, flight Mach number, 0.8.

[redacted]

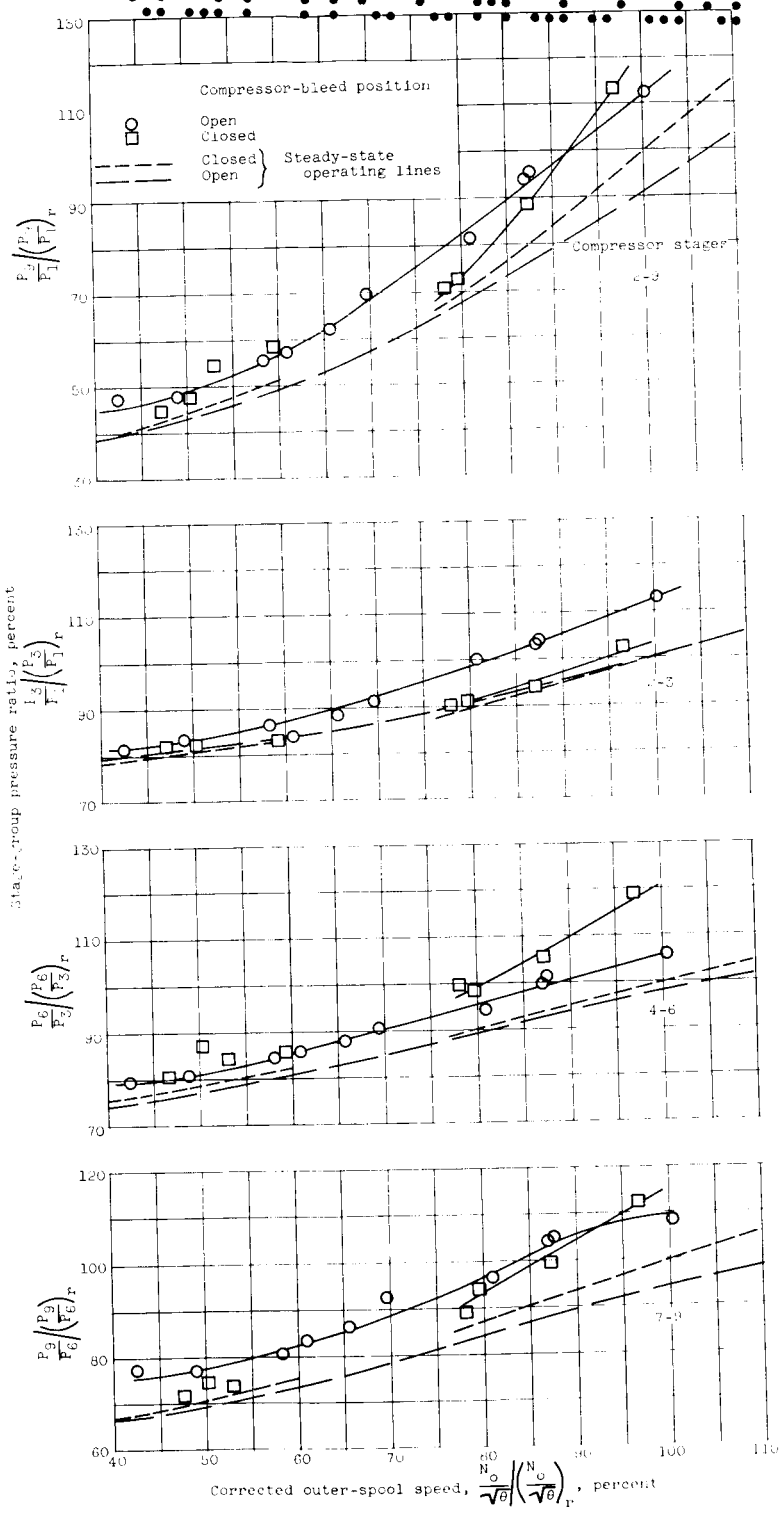

(a) Outer spool.

Figure 21. - Locus of peak stage-group pressure ratios from several accelerations to compressor surge. Altitude, 35,000 feet; flight Mach number, 0.8.

[redacted]

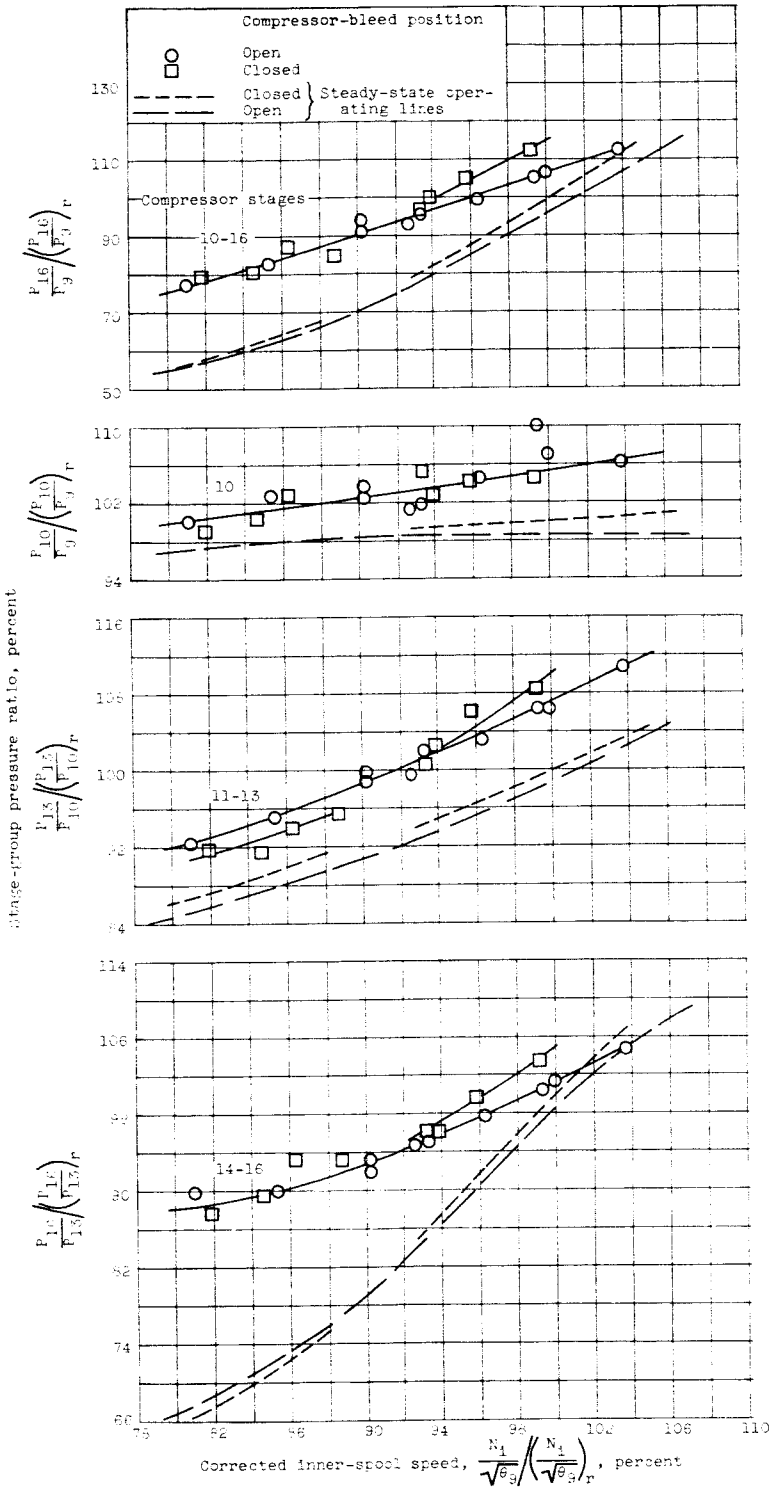

(b) Inner spool.

Figure 21. - Concluded. Locus of peak stage-group pressure ratios from several accelerations to compressor surge. Altitude, 35,000 feet; flight Mach number, 0.8.

[redacted]

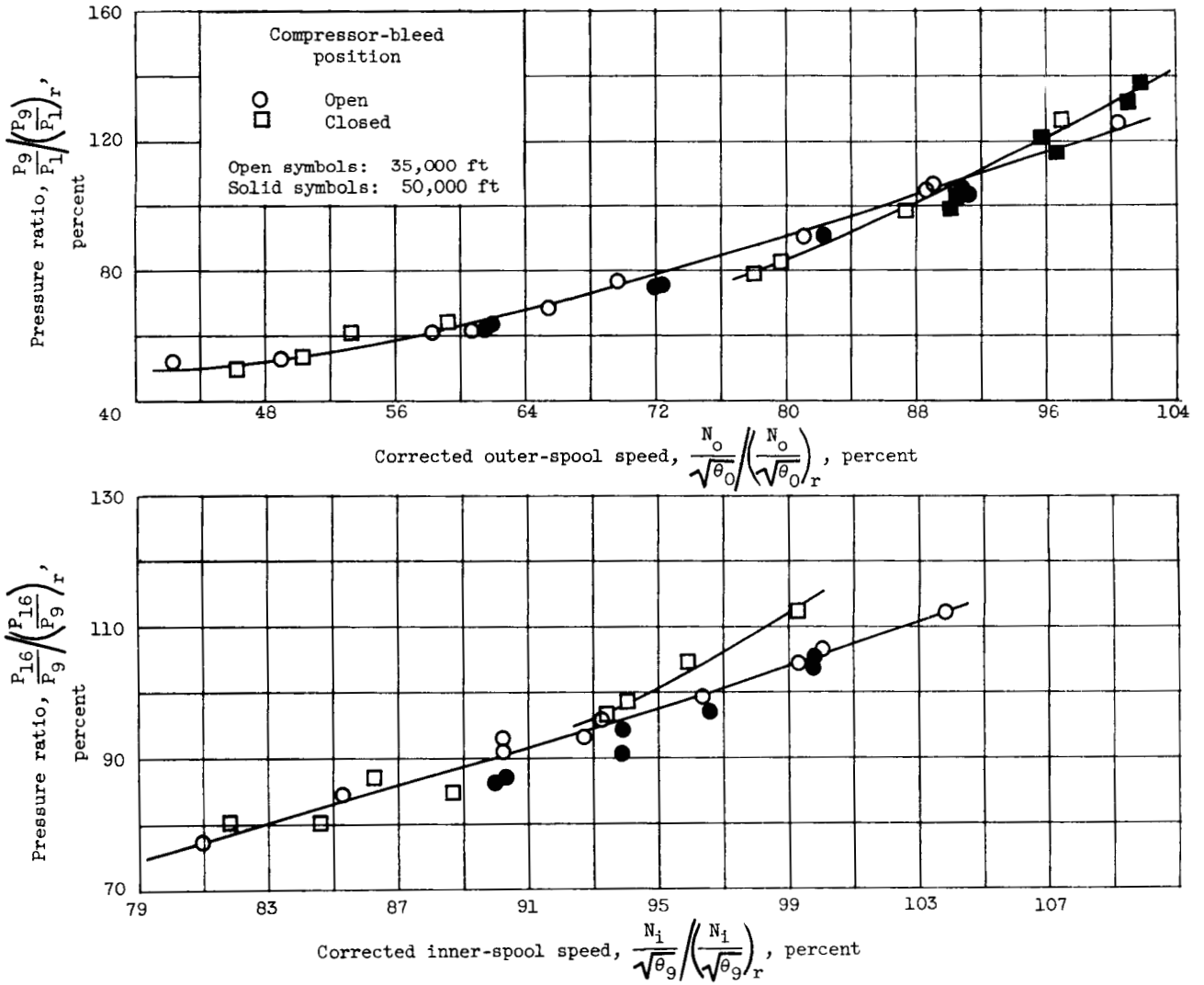

Figure 22. - Effect of altitude on peak compressor pressure ratios from acceleration to compressor surge.

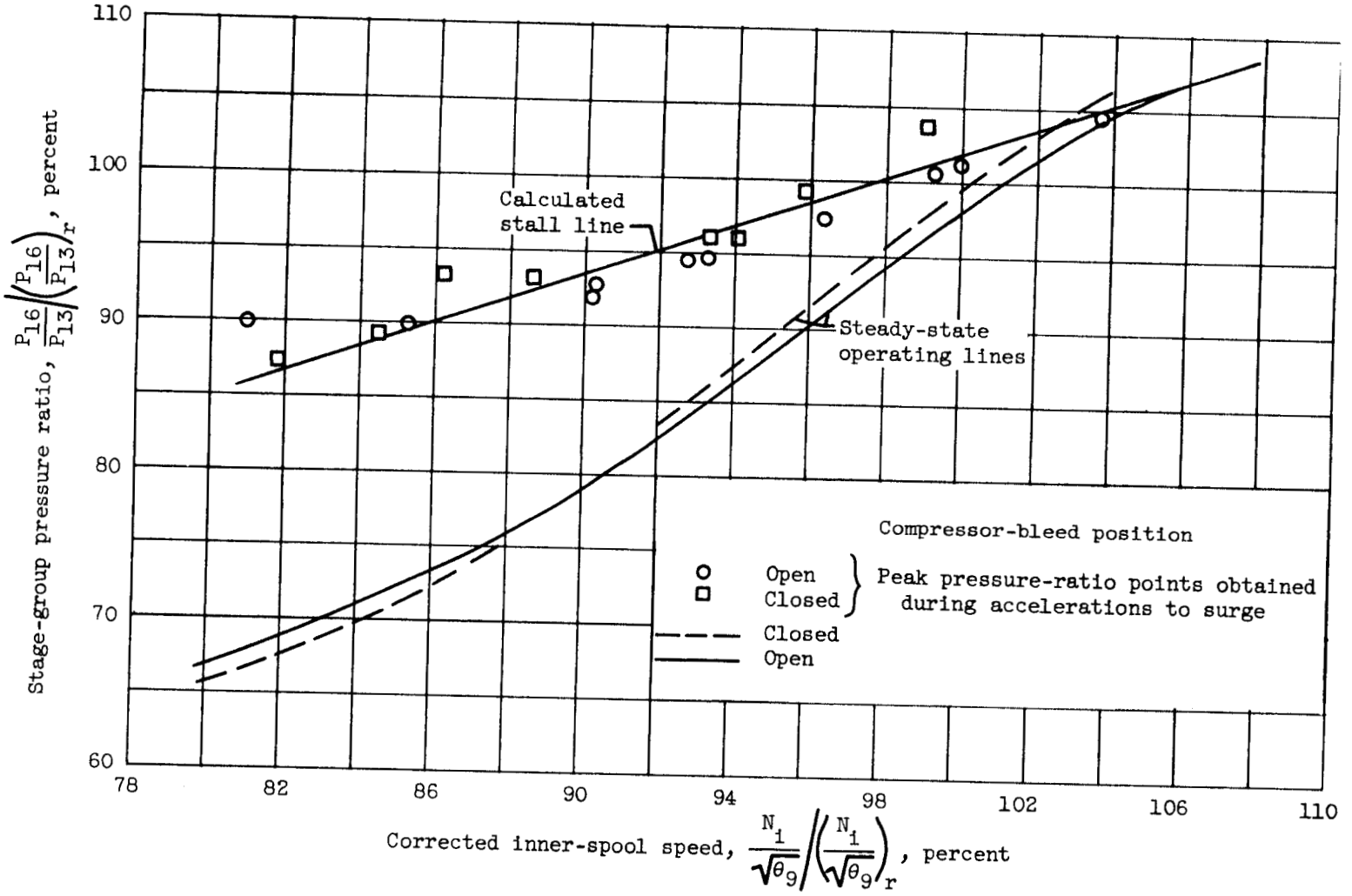

Figure 23. - Comparison of peak stage-group pressure ratios with stage stall line calculated from single peak pressure coefficient value. Altitude, 35,000 feet; flight Mach number, 0.8.

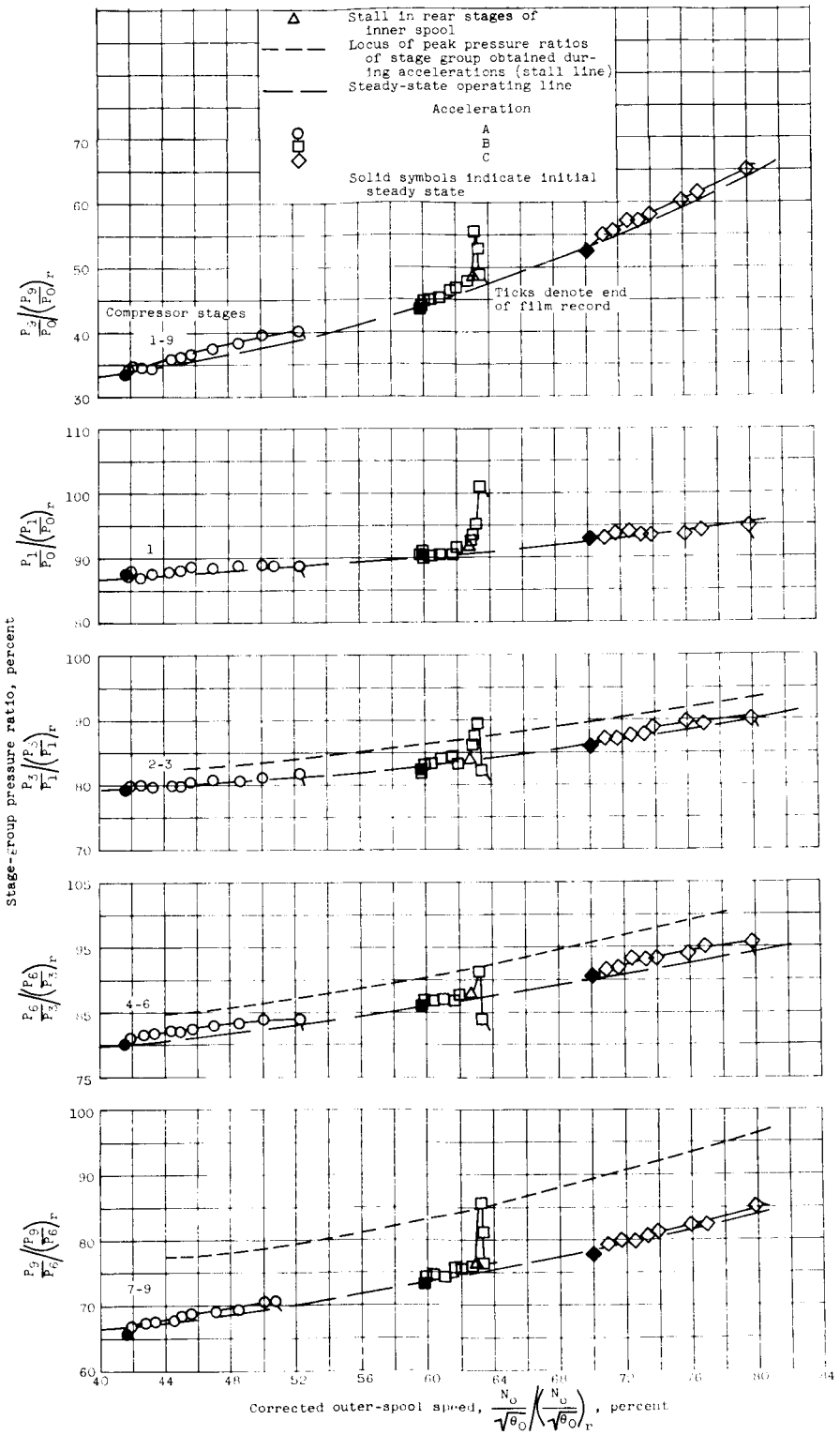

(a) Outer spool.

Figure 24. - Variation of stage-group pressure ratios with speed during several accelerations. Altitude 35,000 feet; compressor bleeds open.

[redacted]

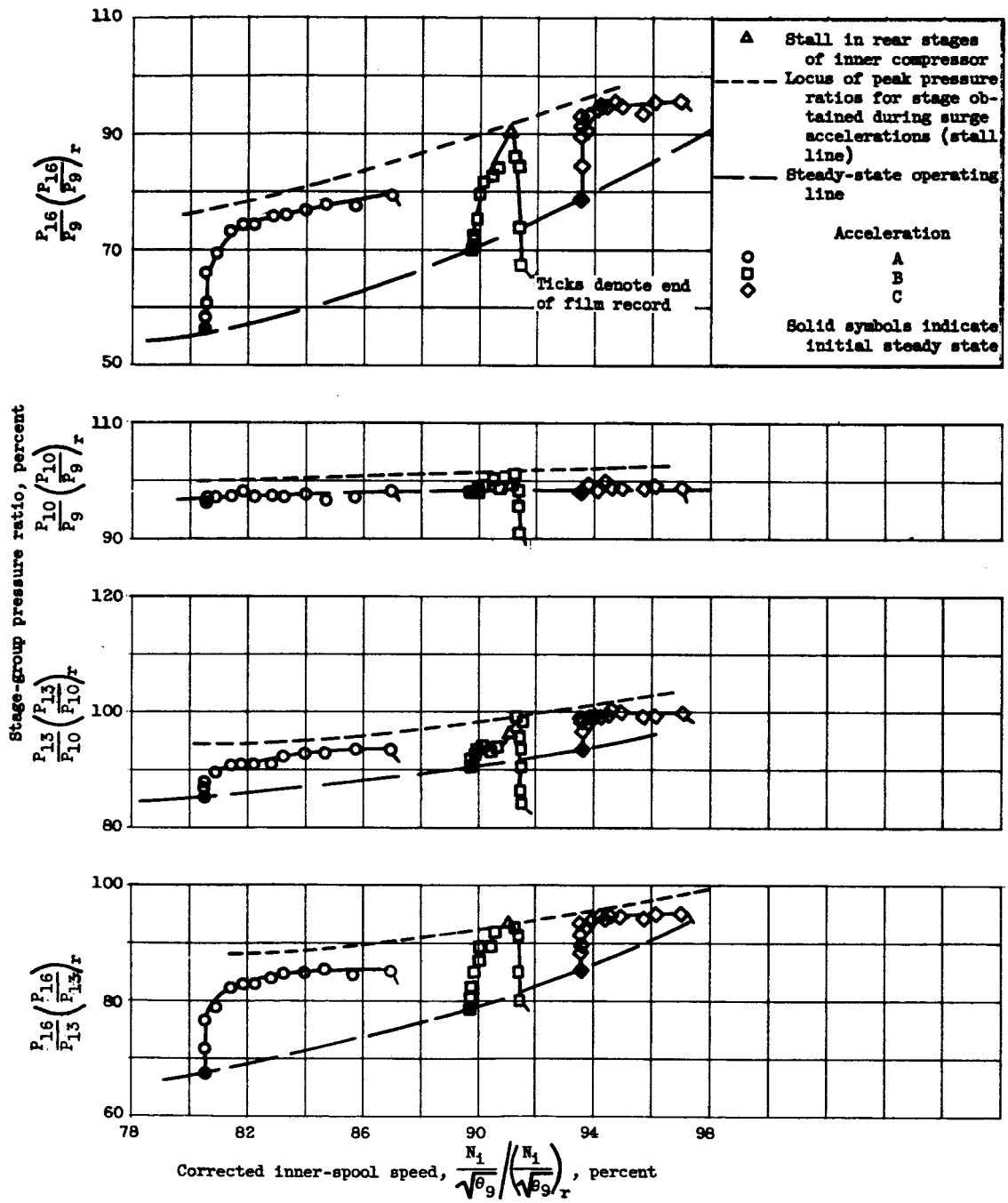

(b) Inner spool.

Figure 24. - Concluded. Variation of stage-group pressure ratios with speed during several accelerations. Altitude 35,000 feet; compressor bleeds open.